Gamma-ray Emission From Dark Matter Annihilation Process In Simulated Coma Like Galaxy Cluster

By

Goshu Woldeyesus Damte

A THESIS SUBMITTED TO

GRADUATE PROGRAMS OF
ADDIS ABABA UNIVERSITY

IN PARTIAL FULFILLMENT FOR THE REQUIREMENTS
OF THE DEGREE

MASTER OF SCIENCE IN PHYSICS

(ASTRONOMY/ASTROPHYSICS)

ADDIS ABABA, ETHIOPIA

OCTOBER 2018

Addis Ababa University
Program of Graduate Studies

Gamma-ray Emission From Dark Matter Annihilation Process In Simulated Coma Like Galaxy Cluster

By
Goshu Woldeyesus Damte
Deparment of Physics
Addis Ababa University

Approved by the Examining Board:

Dr. Remudin Reshid Advisor	______________________ Signature
Dr. Teshome Senbeta Examiner	______________________ Signature
Dr. Getinet Feleke Examiner	______________________ Signature

Date: October 2018

ADDIS ABABA UNIVERSITY

Date: **October 2018**

Author: **Goshu Woldeyesus Damte**

Title: **Gamma-ray Emission From Dark Matter Annihilation Process In Simulated Coma Like Galaxy Cluster**

Department: **Deparment of Physics**

Degree: **M.Sc.** Convocation: **September** Year: **7**

Permission is herewith granted to Addis Ababa University to circulate and to have copied for non-commercial purposes, at its discretion, the above title upon the request of individuals or institutions.

____

Signature of Author

This Work is Dedicated

to Enat Tefera

Table of Contents

Table of Contents **v**

List of Table **vii**

List of Figures **viii**

Acknowledgements **x**

Abbreviations **xi**

Physical Constants **xiii**

Symbols **xiv**

Abstract **xv**

1 Introduction **1**

2 Dark Matter and Non-thermal Process in Galaxy Cluster **4**

2.1 Introduction 4

2.2 The history of DM 4

2.3 Evidence for DM 5

2.3.1 Virial theorem 6

2.3.2 Rotational curve of galaxy 6

2.3.3 Bullet Cluster 8

2.4 Properties of DM 10

2.5 DM candidates 12

2.5.1 Massive astrophysical compact halo objects (MACHOs) 12

2.5.2 Weakly interacting massive particles (WIMPs) 13

2.6 The DM problem 15

2.6.1 DM in galaxy 15

2.6.2 DM in galaxy clusters 16

2.7 DM detection strategies 18
2.7.1 Particle colliders 19
2.7.2 Direct detection strategies 21
2.7.3 Indirect detection strategies 22
2.8 Non-thermal processes in galaxy cluster 23
2.9 The source of the relativistic particles and gamma-ray in galaxy cluster 24
2.10 The source of relativistic particles from galaxy cluster 24
2.10.1 Secondary electrons 24
2.10.2 Secondary electrons from DM annihilation process 25
2.11 Summary 27

3 Methodology and Data Presentation **29**
3.1 Introduction 29
3.2 Data presentation 29
3.3 Modeling the gamma-ray emission 30
3.3.1 The equilibrium spectra of emitting particles 30
3.3.2 The gamma-ray flux from pion decay 32
3.3.3 Gamma-ray emission from ICS processes 32
3.3.4 The gamma-ray emission from non-thermal Bremsstrahlung radiation 33
3.4 Data analysis 34
3.5 Summary 35

4 Result And Discussion **36**
4.1 Introduction 36
4.2 Distribution of DM within the galaxy clusters 36
4.3 Density profile of one specific cluster 38
4.4 The distribution of DM in different galaxy clusters 39
4.5 Gamma-ray flux and emission maps 40
4.6 Differential gamma-ray flux density 43
4.7 Summary 47

5 Conclusion **49**

Bibliography **51**

List of Tables

4.1 Pion decay and non-thermal Bremsstrahlung for the minimum and maximum photon energy and differential gamma-flux for three galaxy clusters SGC280, SGC281 and SGC282. 47

List of Figures

1.1 Graphical representation of multi-wavelength emission from neutralino annihilation processes 2

2.1 The observed rotational speed of M33 galaxy in comparison with what is expected from its luminous disk [2] and [3] 8

2.2 Distribution of matter in the Bullet Cluster. The smaller cluster (blue region on the right) is seen to emerge from the larger cluster (blue region on the left) consequently stripped the system's X-ray emitting hot gas (red color) taken from [4]. 9

2.3 Color-coded temperature map superposed on the contour map of the total band. The positions of four bright galaxies are indicated with crosses. The temperature map of the Coma cluster [5] 17

2.4 DM have four complementary approaches: direct detection, indirect detection, particle colliders, and astrophysical probes. The lines connect the experimental approaches with the categories of particles that they most stringently probe. The diagrams give example reactions of DM with standard model particles (SM) for each experimental approach.. 19

2.5 Constraints in the (m_χ , Ω_χ) plane from the LHC and the International Linear Collider, and from the WMAP [7] and WMAP and Planck measure Ω_χ , but are insensitive to the DM mass m_χ, the collider experiments bound both. These results are for LCC1, a supersymmetric model with minimal supergravity parameters Planck satellites . . . 21

4.1 The DM density square map of Galaxy Cluster (SGC281) and Galaxy Cluster (SGC282) in Fig a and b respectively are obtained using SPH kernel. 37

4.2 The density profile of DM, gas and stars in red solid , green dotted and bluedot dashed curve, respectively [7] 38

4.3 Comparision of DM densities binned on log-scale r from three galaxy clusters 40

4.4 Gamma-ray emission map from pion decay and non-thermal Bremsstralung for SGC280 at 9 MeV in a and b, respectively. 41

4.5 Gamma-ray from pion decay processes at 1 MeV and 100 MeV for SGC280 in Fig a and b. 41

4.6 Gamma-ray emission from pion decay processes at 100 MeV for SGC281 and SGC282 in Figs. 4.5 a and b, respectively. 42

4.7 Differential gamma-ray flux densities from neutral pion decay in the three galaxy clusters SGC280, SGC281 and SGC282 with blue, red dot dashed and green curve, respectively 43

4.8 Differential gamma-ray flux densities from neutral pion decay and non-thermal Bremsstrahlung in three galaxy clusters SGC280, SGC281 and SGC282 with black, magneta and green dot dashed curve, respectively 44

4.9 Differential gamma-ray flux densities from pion decay, non-thermal Bremsstrahlung and IC scattering processes for SGC280 is given in the plot with red dot dashed, blue dashed and pink solid curve, respectively. 45

Acknowledgements

Before I begin, I would like to thank my God. This work would not have been possible without the help of God, who has surrounded me with all of these fantastic people, as well as for providing me the ability and opportunity to do what I want with my life.

This thesis work would have not been accomplished without the support and guidance of my advisor, Dr. Remudin Reshid. I feel very lucky to have had Dr. Remudin as my advisor. With his excellent guidance, assistance, and contribution of valuable suggestions this work would have not been possible.

Most of all, I would like to thank my family with special thanks to my dearest brothers Dessalegn and Habtamu. Their financial support and provision of important materials for my thesis is highly appreciated.

I am also gratefull to my classmates. Particularly Fistum W/Gerima for his various useful comments and advise and Abdu Seid for showing me latex writting teachniques software that helped me while writting my paper.

Last but not list, I wish to express my gratitude to the department of physics, Addis Ababa University and all my instructors.

Addis Ababa University | Goshu Woldeyesus Damte
September, 2018

Abbreviations

WIMPs	Weakly Interacting Massive Particles
ICM	Intera Cluster Medium
DM	Dark Matter
SM	Standard Matter
ICS	Inverse Compton Scattering
LHC	Large Hadron Collider
NFW	Navarro-Frenk-White
AGN	Active Galactic Nuclino
HDM	Hot Dark Matter
MACHO	MAsive Compact Halo Object
ACDM	A Cold Dark Matter
SPH	Smooth Particle Hydrodynamics
CTA	Cherenkov Telescope Array

MUSIC	MUltiDark SImulation of galaxy Clusters
SGC280	Simulated Galaxy Cluster 280
SGC281	Simulated Galaxy Cluster 281
SGC282	Simulated Galaxy Cluster 282

Physical Constants

Speed of Light	C = 2.99792458×10^{8} ms^{-2}
Mass of an Electron	Me = 9.10938356×10^{-28} g
Mass of Proton	Mp = 1.67262178×10^{-24} g
Mass of the Sun	$M\odot$ = 1.99×10^{33} g
Kiloparsec	kpc = 3.08568025×10^{21} cm
Boltzmann constant	k = 1.3806505×10^{-23} JK^{-1}
Thomson cross section	σ_t = 6.652×10^{-25} cm^2

Symbols

$\frac{dF}{dE}$	Differential flux ph. cm^{-2} s^{-1} GeV^{-1}
M_χ	Neutralinos Or DM mass GeV
ρ_{DM}	DM density $M_\odot$ kpc^{-3}
ρ_{GAS}	Gas density $M_\odot$ kpc^{-3}
n_{el}	Number density of Electrons cm^{-2}
D_l	Luminosity distance of the Coma cluster 96 Mpc

Abstract

Galaxy clusters are good targets to search for signals from dark matter (DM) annihilation process as they are dominatly composed of DM. From DM annihilation process neutral and charged pions are beleived to be produced. The neutral pions decay directly into gamma-rays, while the secondary particle $e^{\pm}$ produced from the charged pions are expected to emit gamma-rays through inverse compton scattering (ICS) and non-thermal bremsstrahlung processes. Taking energetic particles that are $e^{\pm}$ produced from DM annihilation process for the model of the origin of the extended secondary particle observed in radio halos, the corresponding gamma-ray emission in those regions, we have studied both their morphology and the spectral energy distribution using simulated Coma like galaxy clusters. Using raw galaxy cluster data from large set of MUltiDark SImulation of galaxy Clusters (MUSIC-2) dataset simulation we choose three galaxy clusters for calculating gamma-ray emmission from DM annhilation process. For our calculation we have considered a neutralino annihilation of $b\bar{b}$ species and mass of DM model of neutralino mass of 35 GeV with annihilation cross-section times velocity of $<\sigma v> = 1\times 10^{-26}$ cm^3 s^{-1}. Among the three simulated galaxy clusters, simulated galaxy cluster SGC282 showes the densest DM distribution almost in all the regions of the map. The differential gamma-ray flux obtained from neutral pion decay process is on average an order of magnitude higher than that from non-thermal Bremsstrahlung process, for similar photon energy, for all the three simulated galaxy clusters. For all the three gamma-ray emission mechanisims from DM annihilation process, simulated galaxy cluster SGC282 showes dominant differential gamma-ray flux densities. Overall we have observed that the gamma-ray emission flux calculated in these simulated galaxy cluster from the DM annihilation process is higher from regions of denser DM halos in the simulated Coma like galaxy cluster as expected.

CHAPTER 1

Introduction

Astrophysics provide several convincing evidences of the existence of DM [8]. Clusters of galaxies are the most massive virialized objects in the universe. About 80% of the mass of clusters is comprised of DM, making them good candidates for astrophysical searches for a signature from particle DM. Among the best motivated particle candidates for DM are weakly interacting massive particles, or "WIMPs". Their annihilation and decay gives standard matter (SM) particles, including electrons and positrons[10].

Annihilation signatures, especially gamma rays, have been searched for in regions where the DM density is expected to be high, as annihilation rate is proportional to the density squared [9]. A type of cold DM particles which are WIMPs known as neutralinos are believed to constitute DM. The neutralinos are Majorana type particles, hence they are their own anti-particles. Thus their annihilation is expected to produce SM-particles such as neutral and charged pions (see. Fig. 1.1). Neutral pions and charged pions will decay into gamma-rays and relativistic electrons/positrons, respectively in relatively short time. These secondary electrons/positrons for example will also produce gamma-rays from bremsstrahlung radiation and ICS processes [7].

The case of the radio halo and relics observed in galaxy cluster models bassed on DM annihilation process were put forward, however these models for example were not able to produce the exact radio halo distribution (morphology) as they model the DM in the cluster as a single main spherically symetric halo. So we use high resolution cosmological simulation which allow us to determine both the morphology of non-thermal emission region and the specteral feature in the Coma like galaxy cluster. Therefore this motivates us to study this work. Our work is basically to studies the morphology, the spectral profile and the DM distribution in three simulated Coma like galaxy clusters (GC280, GC281 and GC282).

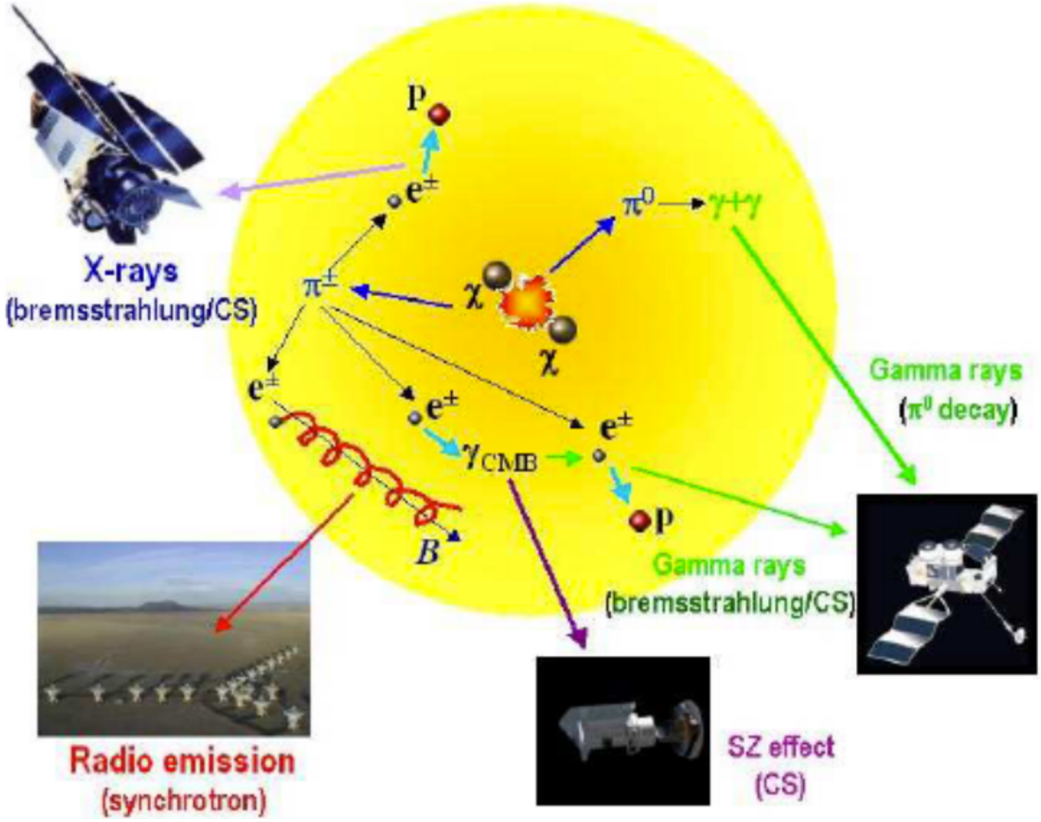

Figure 1.1: Graphical representation of multi-wavelength emission from neutralino annihilation processes

[1].

The objective of this work is to obtain (predict) gamma-ray emission from DM annihilation process in simulated Coma like galaxy cluster. To study the DM distribution in the spectral profile for simulated Coma like galaxy clusters and its differential gamma-ray flux densities. To produce the gamma-ray emission maps at different photon energy by using the neutral pion decay, non-thermal bremsstrahlung and IC scattering process.

The organization of the thesis will be as follows:- We will introduce gamma-ray emission from DM annihilation process in simulated coma like galaxy cluster and the main objecties of our work in the first Chapter. In Chapter two the gamma-ray emission from galaxy clusters and different models for the possible sources of the relativistic electrons which are responsible for the gamma-ray emission emission are broadly discussed. Where as in Chapter three we present the modeling for the gamma-ray emission with the proper mathematical formulation of the magnetic field strength, the "electron equilibrium spectra", the local emissivity and ultimately the gamma-ray flux. We conclude Chapter three by introducing our data sources and the simulation techniques followed to analyse our data. In Chapter four the results (maps and graphs) obtained from the simulation and their elaborate discussions are presented. Finally, we gave conclusion of our work in Chapter five.

CHAPTER 2

Dark Matter and Non-thermal Process in Galaxy Cluster

2.1 Introduction

In this chapter we will give general information of DM such as; to develop the evidence of DM, to know which DM candidate is more approprete for our study and to search the orign of gamma-ray. Quite a number of evidences exist in modern cosmology to inform us that the ordinary baryonic matter, which is the usual form of matter in diffuse gas, stars and galaxies, make up only 5% of the Universe. The remaining 95% of the matter in the Universe is still in an unidentified form. Of this nearly 70% is contributed by dark energy and the remaining 25% is DM in galaxy cluster. Clusters of galaxies are the largest gravitationally bound systems in the Universe, with typical masses of about 10^{15} $M_{\odot}$, and volumes of about 100 Mpc^3. This thermal plasma, consisting of particles of energies of several keV, is commonly referred to as Intracluster Medium (ICM). Clusters are formed by hierarchical structure formation processes. In this scenario, smaller units (galaxies, groups and small clusters) formed first and merged under gravitational pull to larger and larger units in the course of time.

2.2 The history of DM

During the last 70 years, a new paradigm has emerged in which the matter visible to us in current telescopes only represents a small fraction of the total amount present in the Universe. Most of the matter instead appears to be in some form which does not emit light, or at least very little. This is what is referred to as DM. To this day, the nature of this elusive component of the Universe remains a mystery [11].

The discovery by [12] that visible matter accounts for only a tiny fraction of all of the mass in the universe may turn out to have been one of the most profound new insights produced by scientific exploration during the 20^{th} century [13]. From observations of the radial velocities of eight galaxies in the Coma cluster, Zwicky found an unexpectedly large velocity dispersion, σ = 1019 $\pm$360 km s^{-1} (if the most deviant galaxy is rejected as a for ground object, the velocity dispersion becomes σ = 706 $\pm$ 267 km s^{-1}). It is noted in passing that Zwicky's velocity dispersion from only eight galaxies agrees well with the modern value, σ = 1082 km s^{-1} obtained by [14]. Zwicky concluded from these observations that, for a velocity dispersion of 1000 km s^{-1}, the mean density of the Coma cluster would have to be 400 times greater than that which is derived from luminous matter. Zwicky overestimated the mass-to-light ratio of the Coma cluster because he assumed a Hubble parameter H_o= 558 km s^{-1} Mpc^{-1}. His value for the overdensity of the Coma cluster should therefore be reduced from 400 to $\sim$ 50 [15].

Zwicky writes : " if this (overdensity) is confirmed we would arrive at the astonishing conclusion that DM is present (in Coma) with a much greater density than luminous matter". Assuming that M31 and the Galaxy started to move apart 15 Gyr ago, these authors found that the mass of the Local Group had to be $\gtrsim$ 1.8 $\times$ 10^{12} $M_{\odot}$. Assuming that the combined mass of the Andromeda galaxy and the Milky Way system was 0.5 $\times$ 10^{12} $M_{\odot}$, [16] concluded that most of the mass of the Local Group existed in some invisible form. They conclude that it was most likely that this missing mass was in the form of DM.

Once it was recognized that most of the matter in the Universe was dark, this component was expected to dictate the conditions for the formation of large structures like galaxies and galaxy clusters. The fact that relativistic DM particles (i.e. moving close to the speed of light in the early Universe) today referred to as hot dark matter (HDM) like standard, low-mass neutrinos, would have severe trouble in explaining the observed structures soon became evident.

2.3 Evidence for DM

Most of our knowledge of the Universe comes from electromagnetic waves emitted by astronomical objects. DM on the other hand, does not interact with the electromagnetic spectrum. It is completely invisible, it does not emit, absorb or reflect light at any frequency. In fact, it does not interact with ordinary matter at all, and hence it is very difficult to detect. The evidence that DM actually exists comes from its gravitational effect on other objects that we can observe. Visible matter behaves in ways that cannot be explained in standard gravitational theories without additional, invisible matter [17]. Given the strength of the evidence that most of the matter in the Universe is DM, what can be done to discover it and study its properties? [18].

2.3.1 Virial theorem

[1] The time a galaxy needs to travel through the cluster is much smaller than the age of the Unverse, therefore it can be assumed that clusters of galaxies are relatively bound systems. The cluster is in virial balance

$$T = -\frac{1}{2}U, \tag{2.1}$$

where T and U are kinetic and potential energies, respectively of the system. The single mass, as well as the single velocity can not be measured directly. It has to be assumed that the system is spherically symmetric and in equilibrium, so that the velocity is uniformly distributed over all directions. V^2 is velocity square [19]. The kinetic energy equals to

$$T = \frac{1}{2}MV^2 \tag{2.2}$$

Analysing the motions of all kinds of clusters shows that they cannot be stable unless there is a lager amount of mass than visible. But Zwicky's discovery was largely ignored. In 1932 he was one of the first to really grasp the significant presence of DM. He called it missing matter. What he did not know then was, whether DM was just dark objects and galaxies that he could not see or whether it was something truly different [19].

2.3.2 Rotational curve of galaxy

It took 50 more years for to study DM. The American astronomer Vera Rubin provided a major contribution to this. She observed the rotation curves of galaxies similar to the Milky Way. Equating gravitational and centripetal force

$$M\frac{V^2}{R} = \frac{GM(R)m}{R^2} \tag{2.3}$$

[1] Virial theorem states that the average kinetic energy of a self-gravitating system in steady state equals half of the average negative potential energy.

and putting it in order to the velocity

$$V^2 = \frac{GM(R)}{R} \tag{2.4}$$

where V-is the averege orbital velocity of planet, G-is the Newton's constant , M(R)-the total mass inside the oribit. Clearly, V decreases with increasing radius since M(R) is constant and given by the solar mass [7].

It proves that the more stuff an object has, the more gravitational pull it should have. And the further an object is from the centre, the slower it should travel in orbit, because the gravitational pull declines, it should be likewise for a galaxy. Within the bulge the density is almost constant and the mass increases with the cube of the radius. In the bulge the rotational velocity increases linear to the radius, while in the disc the mass is constant. A decline of the curve is to be expected. The theoretical curve should therefore look like the disk in Fig. 2.1 points out the discrepancy between the observed and expected radial velocity curve for the galaxy M33 [3].

The missing mass is believed to lie in a spherical halo of DM around the galaxy. But Vera Rubin measured that with an increasing distance to the galactic centre the velocity of the orbiting gas and dust remained constant until the visible edge of the galaxy. She concluded that there had to be more mass. Otherwise the galaxy would have fallen apart. The only way to resolve that paradox was to assume that there is a halo of invisible matter surrounding the galaxy [18].

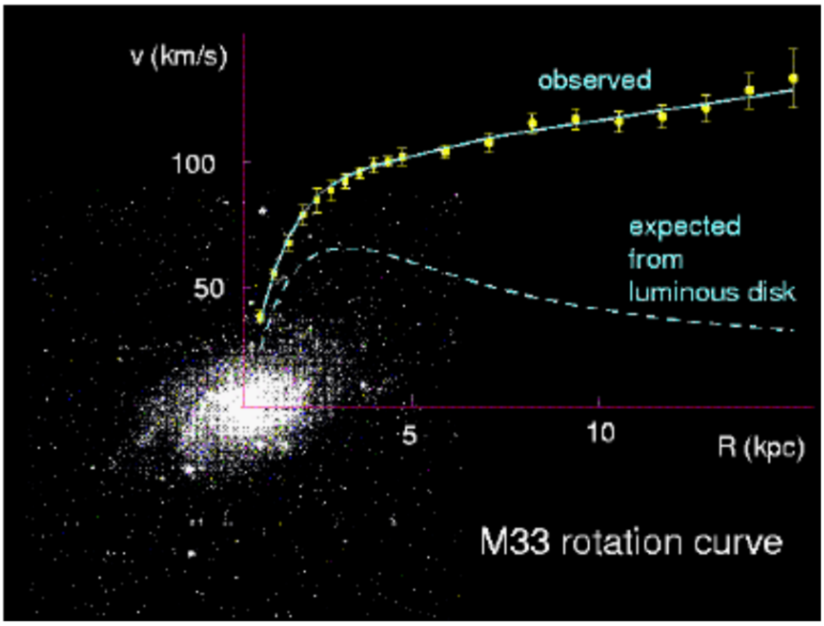

Figure 2.1: The observed rotational speed of M33 galaxy in comparison with what is expected from its luminous disk [2] and [3]

2.3.3 Bullet Cluster

Another important discovery was made in 2006. A clash of two galaxies called Bullet Cluster was observed. Analysing the spectral regions shows that the clash caused a strong separation of the individual components of the galaxy clusters. The stars and galaxies passed each other without interaction. The homogeneously distributed gas clouds interacted significantly and created the bullet like image Fig. 2.2. The maxima of the gravitational potential is not on the maxima of the visible matter density. Therefore there has to be an additional contribution of DM. The lager amount of matter is at the position of the galaxies and not, as expected, with the more massive gas clouds. Before the clash, the DM was homogeneously distributed in the galaxies as well as in the gas clouds. But while the gas interacted due to the crash the DM did not, neither with itself nor with others. It travelled trough the gas clouds, which were slowed down [20].

The "Bullet Cluster" is composed of two massive clumps of differing mass, that have undergone collision. As shown in Fig.2.2 we see a smaller cluster (right region in blue color) emerging from larger cluster (left region in blue color) after a high-speed collision which has separated the X-ray emitting hot gas (indicated in red color) from that of the galaxies [21]. A map of the system's overall mass (indicated in blue color) made from gravitational lensing observations [22], does

Figure 2.2: Distribution of matter in the Bullet Cluster. The smaller cluster (blue region on the right) is seen to emerge from the larger cluster (blue region on the left) consequently stripped the system's X-ray emitting hot gas (red color) taken from [4].

not coincide with the location of the system's hot gas which is obtained through X-ray observations (indicated in red color) [21].

This fact is difficult to explain without the inclusion of DM, because the gas contains several times as much mass as all the cluster's stars combined. An easiest explanation for this morphology of Bullet Cluster is, however possible, if DM is to be included, i.e., the collision has simply stripped the hot gas away from the DM on which it was previously centered. Moreover, the "Bullet Cluster" is not the only galaxy cluster where the distribution of DM derived using the gravitational lensing technique is found to be quite different from the X-ray one, another case for example is that of A1914 [23].

2.4 Properties of DM

Cosmological parameter estimation, based on cosmic microwave background anisotropies measured by the WMAP satellite [24] and based on the power spectrum of galaxy density fluctuations measured by the Sloan Digital Sky Survey (SDSS) collaboration [25] indicates that most of matter in the universe is unobserved save by gravity. DM is an elusive form of matter that comprises 84.5 % of the mass of the Universe (DM is 23 %, luminous matter or baryonic matter is 4 %¸, and dark energy is 73% of the total mass-energy density. Telescopes cannot observe it directly as it does not interact electromagnetically, but we can infer its presence from its gravitational effects on neighboring stars and galaxies. The DM and dark energy are unknown composition.

i. Optically Dark (Dissipationless):- DM is not observed to shine, thus the DM particles must have very weak electromagnetic interactions. Either the electric charge and electric and magnetic dipole moments must vanish (or be very small), or the particles must be very heavy. For a review of constraints on DM from background light across the electromagnetic spectrum [26].
An important consequence of this is that the DM cannot radiating photons, and thus will not collapse to the center of galaxies as the baryons do, by radiating their energy away electromagnetically.

ii. Collision-less:- DM is "nearly collision-less" i.e., the interaction cross-section between DM and baryonic matter for densities found in DM halos is so small to be considered negligible. This also means that its particles are only gravitationally bound to one another and travel unimpeded in orbits in the halos with a broad spectrum of eccentricities [7].

In addition to not interacting with "light" matter (to ensure that energy is not dissipated), the DM must be nearly collisionless as well. Even if the DM can not radiate energy, collisions will serve to make halos round, in contrast to data that overwhelmingly indicates triaxiality, e.g. in clusters. The limit of this constraint is that there can be DM self interactions that are important at high densities and short distance scales, which may serve to erase small scale structure in galaxy halos, and erase the density cusps expected at the cores of galaxies.

iii. Cold:- DM is "cold", which means that they move at non-relativistic speed as they enter matter-dominated era and to cluster effectively and produce the observed intricate structures we observed [7]. In the early 1980's it was noted that 'cold' DM explained the observed properties of galaxies quite well [27]. The measured two point correlation function of galaxies indicates that there is a large amount of power on small scales. If the DM particles have significant velocities, then the small scale power is erased. For this not to occur, the particles must be sufficiently non-relativistic at the epoch of matter-radiation equality [28]. In practice, the constraint is that a particle species in thermal equilibrium must have a mass larger than about 1 keV [29]. Of course, a non-thermal species can have a smaller mass [30].

iv. Fluid:- The DM must be sufficiently fine on galaxy scales such that the discreteness is not detectable as yet. There are two basic effects to be concerned with this. The first is that charterastic of DM provides a time dependent gravitational potential, which may disrupt bound systems. For particles of 10^6 $M_\odot$, this effect would heat the galactic disk to observable levels, while globular clusters would be disrupted for smaller masses, around 10^3 $M_\odot$ [31]. Second, the discreteness of DM introduces Poisson noise in the power spectrum of density fluctuations, which conflicts with observations of the Lyα forest if the particles are more massive than roughly $m \gtrsim 10^4$ $M_\odot$. We thus find that an upper bound on the mass of particles of roughly $M \lesssim 10^{3-4}$ $M_\odot \sim 10^{70-71}$ eV. Gravitational microlensing places further constraints on DM in the solar mass range. Searches for lenses by the MACHO and EROS collaborations have failed to find enough microlensing events to explain the full dark halo of the Milky Way [32], though MACHO reports that 2% of the Milky Way halo consists of objects of roughly 0.3 $M_\odot$. The constraints are that objects between 10^7 $M_\odot$ and 10 $M_\odot$ do not make up more than about 20%¸ of the DM in the Milky Way halo. Microlensing surveys are not able to place constraints much outside this mass range due to the limitations of microlensing event timescales.
v. Stable:- DM is "stable" which means that its lifetime must be comparable to the age of the Universe. Moreover DM behaves classically to be confined on galaxy scales through attractive gravitational interactions; and as a fluid on galaxy scales as its discreteness is not proved yet [33][7].

i. Classical:- DM must behave sufficiently classically to be confined on galaxy scales. Bounds can be placed on the masses of both bosons and fermions, based only on the observed properties of galaxies: namely galaxy densities must reach of order GeV cm^3, their velocity dispersions are of order 100 kms^1 , and their sizes are of order kpc.[34],[35]

2.5 DM candidates

Here, some of the DM candidates that have been discussed in this section. A substantial part of the DM literature around two important acronyms, WIMPs and MACHOs.

2.5.1 Massive astrophysical compact halo objects (MACHOs)

The MACHOs are large astrophysical objects with masses substantially larger than those of WIMPs. Although the acronym was originally proposed with baryonic objects like failed stars in many nonbaryonic candidates can in fact behave as MACHOs. Therefore, contrary to a wide spread misconception in the astronomical community, the MACHO populations that can be probed through microlensing effects are not necessarily subject to constraints on the baryonic mass fraction of the Universe, and can in principle constitute all of the DM (although current constraints make this seem unlikely). Certain kinds of MACHOs could furthermore have a sufficiently small interaction with the baryonic content of the Universe to effectively behave as Cold Dark Matter (CDM) [36].

One commonly suggested possibilities for DM is to assume astrophysical bodies which are of baryonic form called MACHOs as the main candidates [37]. Some examples of MACHOs include Jupiter-like objects, brown dwarfs (failed stars that are unable to start nuclear reaction), low mass stars and dead stars such as white dwarfs, neutron stars, stellar black hole remnants. Statistics acquired based on experiments using gravitational microlensing effect which are sensitive enough to monitor low mass objects to a mass of 10^{-7} $M_{\odot}$

show that MACHOs contribute less than 25% of the mass of DM in the halo of a galaxy [38]. Moreover, the amount of baryonic matter predicted from the big bang nucleosynthesis (BBN) sets an upper limit of Ω_B h^2 ~ 0.02. where Ω_B h relic density [39], which is in agreement with a more recent measurement by Planck experiment of CMB anisotropy [40]. Hence, some of DM could be ordinary matter (MACHOs).

Baryonic candidates

In the standard Big Bang scenario, no more than $\sim$ 1/6 of the cosmic matter density can be attributed to baryons [16]. While making up only a small fraction of the matter in the Universe, this baryonic DM can still be important for understanding. Faint stars and stellar remnants very faint, low-mass stars such as red and brown dwarfs could in principle constitute part of the baryonic DM if located at sufficiently large distances, e.g. in the dark halo of the Milky Way. Brown dwarfs are objects which are too light $< 0.09 M_{\odot}$ to start thermonuclear reactions, whereas red dwarfs are just massive enough 0.09 $< M/M_{\odot}$ <0.2 to burn hydrogen in their cores. Direct searches for the latter have indicated that these contribute less than $1\%_{\text{¸}}$ to the mass of the Milky Way dark halo. The luminosity of brown dwarfs comes from conversion of potential energy into radiation by contraction.

Since this makes them even fainter than red dwarfs, they cannot be detected at equally large distances. To estimate their contribution to the dark halo, a number of assumptions about the stellar intial mass function must be made. Although most studies infer an upper limit on brown dwarfs of the same order as that of red dwarfs, it is in principle possible that the initial mass function may be substantially different at large distances from the Galactic disk. Microlensing surveys do however constrain brown dwarfs to contribute $\leq$ 25% [38] to the mass of the dark halo.

2.5.2 Weakly interacting massive particles (WIMPs)

The WIMPs are small, non-baryonic particles which interact only through gravitational and the weak nuclear force. Their masses are usually assumed to lie in the GeV-TeV range (a proton, by comparison, has a mass of 0.938 GeV and an electron a mass of 0.511 MeV), which would make them sufficiently slow-moving at the time of matter-radiation equality to act as CDM [7].

Because of their lack of strong interaction with normal matter and lack of interaction through electromagnetism, they would appear dark in current telescopes, unless they happen to decay or annihilate into photons. Although there are no known particles within the standard model of particle physics which correspond to WIMPs candidates. The most viable non-baryonic DM candidates are the WIMPs. A compreh- ensive review on this topic can be found in [41][42]. WIMPs are the largest class of cold DM candidates, which are stable particles that arise in extensions of the standard model of electroweak interactions.

Non-baryonic candidates

i. Neutrinos:- Neutrinos represent the only kind of non-baryonic matter which contributes non-negligibly to the cosmic energy density and is actually known to exist. The neutrinos are however constrained by laboratory bounds and the CMBR to be very light ($\sum m_\nu \leq 0.7$ eV), corresponding to a contribution to the cosmic energy budget of $0.001 \leq \Omega_\nu \leq 0.014$. Standard neutrinos in this mass range would act as HDM and are therefore not suitable candidates for the DM of the Universe. A fourth, so-called sterile neutrino which could act as CDM has been postulated from time to time to solve various problems in neutrino physics, but does not seem to be favoured by the most recent experiments [43].

A robust result on the mass constraint of neutrino has emerged from tritium β-decay experiment, which point toward an upper limit of $m_\nu \leq 2$ eV. Neutrino oscillations on the other hand have determined the mass difference Δm between each species (i.e., the electron, muon and tau neutrino) to be Δ m$^2 \sim 3 \times 10^{-3}$ [44]. These two results are then combined to provide the following upper limit for their relic density:

$$\Omega_\nu h^2 \lesssim 0.07. \tag{2.5}$$

This value thus clearly shows that neutrinos cannot be a dominant component of DM [45]. Their mass limit also implies they are relativistic collision-less particles that they would freely stream on scale of about 40 Mpc, as a result of which they would erase the observed density fluctuations on such scale [46]. Moreover simulation results have also shown that the clustering we see today in the Universe cannot fit this picture [47][43].

ii. Axions:- The axion, named after a laundry detergent, was proposed in the late 1970s to blot out a disturbing stain on the face of quantum chromodynamics (QCD), the theory which describes the strong interactions between quarks. The axions favoured as DM candidates interact so weakly that they were never in thermal equilibrium in the early Universe. Because of this, axions would serve as CDM, despite having been constrained to be very light (10^{-6}-10^{-2} eV) [48]. Axions are among well motivated candidates for non-baryonic DM, they were in fact initially proposed not as DM candidates but motivated to solve what is known as the "strong

CP-violation" in QCD [49]. Constraint from various searches in the laboratory and astronomical bounds (such as analysis from supernova observation and stellar cooling) set the mass of axions below 0.01 eV [50]. Several theoretical models suggest that axions should be produced non-thermally in the early universe by mechanisms like the "vacuum realignment" [43][51]. They are expected to have small free-streaming length and interact very weakly with other matter which put them among cold DM candidates. So far masses of axions which pass various cosmology and astrophysical constraints are in a range between 10^{-5} -10^{-2} eV [45]. A comprehensive review on this topic can be found in [43],[52].

2.6 The DM problem

The existence of DM is obtained only indirectly from its gravitational effect on the visible matter, radiation and large-scale structure of the Universe. On small (microscopic) scales DM is believed to show weak interactions and this gives hope that it may be detected in low-energy particle physics experiments. So far there is no direct observation of DM and exactly how much there is, and what it is made of is still under investigation, hence the DM problem remains.

2.6.1 DM in galaxy

Among the most common methods of detecting DM is the gravitational influence it has on the baryonic (visible) matter, which provide us with some useful information regarding its content and distribution. Stars residing in the disk of spiral galaxy (for example galaxies in the local group which the Galaxy and M33 are the member) follow circular path around the center of their host galaxies [7]. Let us consider one of these stars and represent its radius and orbital (rotational) speed by R and v, respectively. Then its acceleration due to the gravitational potential of its host galaxy is given by

$$a = \frac{\upsilon^2}{G} = \frac{GM(R)}{R^2}. \tag{2.6}$$

The rotational speed υ of the star will then be $\sqrt{\frac{GM(R)}{R}}$, which depends on the radius of the orbit R and the mass M(R) accommodated in the spherical region of radius R [2]. If we assume that the stars are contributing dominantly to the mass contained in the galaxy, the orbital velocity is expected to fall off at large radii $\propto R^{-\frac{1}{2}}$.

However, it has been observed that the velocity rises towards a constant value.

For example the rotational speed in the case of M33 is in the range between ~100-200 km s^-1 as shown in Fig.2.1. We deduce that this observed flat rotation curve can only be explained with the presence of some other form of matter "DM" which has extended distribution in the halos of the galaxy.

2.6.2 DM in galaxy clusters

Mass determinations are very important as they measure the amount and distribution of DM in clusters indirectly. The mass of a galaxy cluster can be determined from the "virial theorem" once the three dimensional mean square velocity $< v^2 >$ is obtained from the redshift measurements of a large number of its galaxies, for the case of Coma cluster we have

$$M_{coma} = \frac{< V^2 > rh}{\alpha G} \approx 2 \times 10^{15} M\odot \tag{2.7}$$

where rh and α are the half mass radius of the Coma Cluster and a constant of value $\sim$ 1.0 which depends on the density profile of the cluster, respectively. Comparison of the total mass of Coma cluster with its luminosity (8 $\times$ $10^{12} L\odot, B$) gives a ratio of M_{comma}/L_{comma}, B $\approx$ 250 $\frac{M_\odot}{L_\odot}$, B. This value shows the vast presence of some non-luminous form of matter in the Coma Cluster. This point is also supported by the fact that the hot gas in the central region of the cluster which is observed to emit X-rays is still in place. In other words, if the hot gas was not to be gravitationally bound by the DM, it would have expanded beyond the region of the Coma Cluster on much shorter time scales than the age of the Universe [53].

Observations from the X-ray emitting gas can also be used to trace the gravitational potential in clusters, which thus provide an indirect measure of the amount and distribution of DM in clusters. Let us assume that the hot ICM gas is in hydrostatic equilibrium and it has spherical symmetry. This simplification will allow us to express the mass M(r) contained in the radius r of the cluster only in terms of two quantities, namely the gas temperature T and gas density ρ. Both T and ρ can be inferred from X-ray observations, are used to determine the gas pressure, P , using the ideal gas law

$$P = \frac{\rho k T}{\mu m_p} \tag{2.8}$$

where k is boltzmann constant, μ is the gas particle mass in terms of proton mass m_p. Quantities such as gas temperature and density as well as chemical content can be well determined by fitting the observed X-ray spectrum with theoretical models. An example of this is the temperature map shown in Fig. 2.3 for the case of the Coma Cluster which clearly identifies both relatively hot and cool regions of about kT ~ 12, and 5 keV, respectively with a mean temperature of around 9 keV [5]. In hydrostatic equilibrium, the outward force due to the gas pressure balances

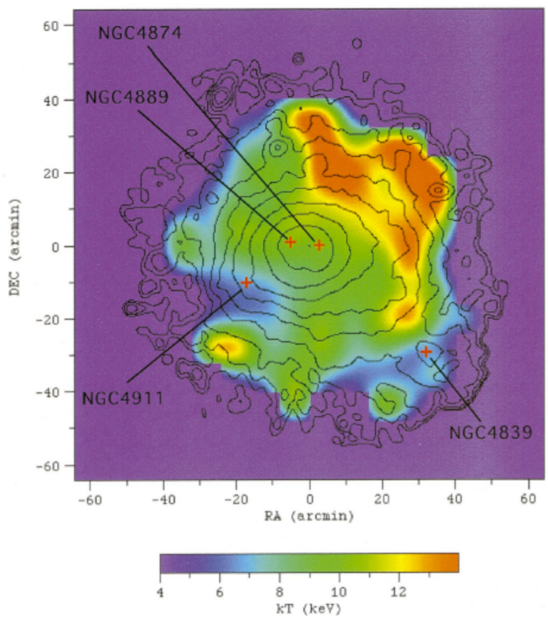

Figure 2.3: Color-coded temperature map superposed on the contour map of the total band. The positions of four bright galaxies are indicated with crosses. The temperature map of the Coma cluster [5]

the force from its gravity infall to give

$$\frac{1}{\rho}\frac{dp}{dr} = -\frac{GM(r)}{r^2} \tag{2.9}$$

If we substitute the gas pressure P, from Eqn.(2.8) in Eqn. (2.9), we obtain the total gravitational mass in the form

$$M(r) = -\frac{kT(r)r}{G\mu m_p}\left[\frac{dln\rho(r)}{dlnr} + \frac{dlnT(r)}{dlnr}\right]. \tag{2.10}$$

Numerical simulations play vital role in advancing our understanding of halo and large-scale structure formation. Their results suggest that the distributions of DM in clusters follow density profile that is power-law. One most commonly used profile is the NFW profile [54] which has the form

$$\rho_{DM}(r) = \rho s\left[\left(\frac{r}{rs}\right)\left(1+\frac{r}{rs}\right)^2\right]^{-1} \tag{2.11}$$

which has flatter appearance at small radii, and a characteristic scale radius r_s (and density ρs) past which they show a sharp decline at large radii. Based on the NFW profile we can express the DM mass $M_{DM}(r)$ contained inside radius r in the cluster by

$$M_{DM}(r) = 4\pi\rho_s r_s^3 \left[ln\left(1+\frac{r}{r_s}\right) - \left(\frac{r}{r+r_s}\right)\right]. \tag{2.12}$$

Observationally the DM mass in the cluster is obtained by subtracting out the mass contained in the form of gas and individual galaxies in the cluster from the total mass of the cluster, i.e.,

$$M_{DM}(r) = M(r) - M_{gas}(r) - M_{gal}(r). \tag{2.13}$$

where $M_{gal}(r)$ is the mass of the galaxies which can be obtained from optical observations and $M_{gas}(r)$ is the mass of the gas, which can be obtained from Eqn.(2.14) once the gas density,$\rho(r)$, is determined by either model fitting or de-projection

$$M_{gas}(r) = 4\pi \int_0^r \rho(r')((r'))^2 dr' \tag{2.14}$$

Results of the mass of the Coma Cluster based on the assumption that the gas is in hydrostatic equilibrium (i.e., using Eqn.(2.10) gives 1-2$\times$ $10^{15}M$)

within 3.6 Mpc radius. We see that this value agrees well with what is determined by applying virial theorem Eqn. (2.7) on its galaxies [53].

Following the same procedure on a large number of clusters it has been found that the typical "mass-to-light ratios" for clusters lie in the range. This indicates the ubiquitous existence of DM in galaxy clusters.

2.7 DM detection strategies

We have seen that a correct amount of DM budget in the universe as observed today can be obtained from a model-independent analysis at the weak scale using WIMPs as a prime candidate. This result has given a strong motivation to the scientific society, which has initiated the development of robust experimental techniques and theoretical frameworks for DM search. A cross-fertilization of these views is thus essential to reach the common goal of detecting DM [55]. We have review the current and projected experiments for detecting WIMPs. For WIMPs χ to have the right relic density, they must annihilate to other particles. Assuming that these other particles are standard model (SM) particles, three most promising detection channels have been put forward. These are, production of DM at the colliders, direct and indirect detection of DM which will be described briefly in the following sub-sections. Schematic representation of these three possible DM detection strategies show in Fig 2.4 [56] adopted from Fig 2.4

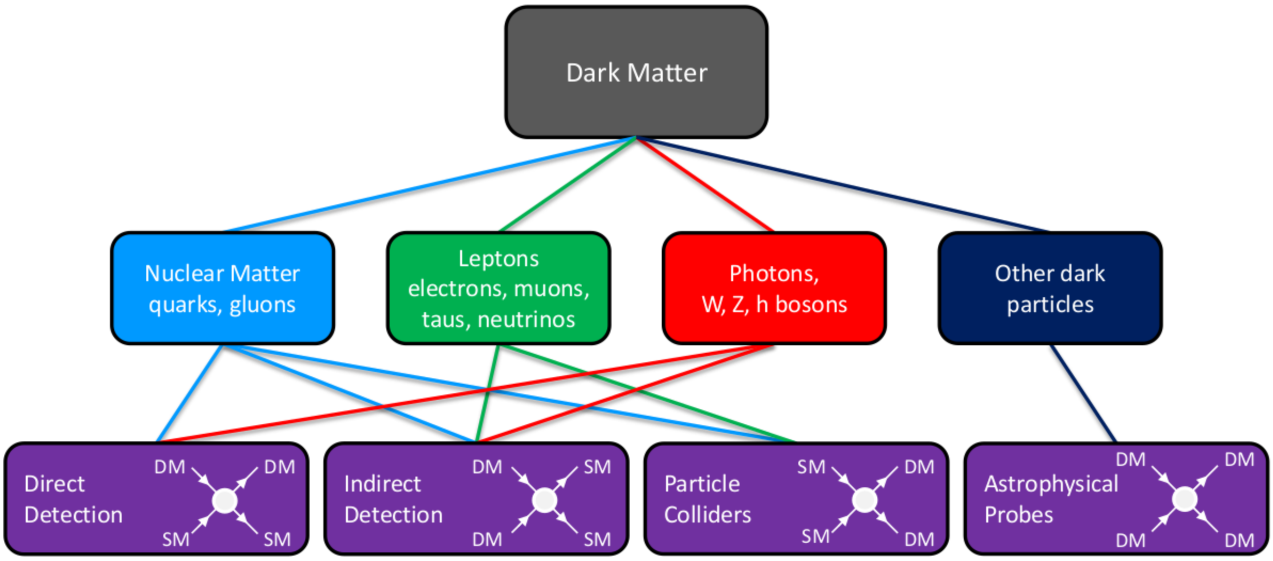

Figure 2.4: DM have four complementary approaches: direct detection, indirect detection, particle colliders, and astrophysical probes. The lines connect the experimental approaches with the categories of particles that they most stringently probe. The diagrams give example reactions of DM with standard model particles (SM) for each experimental approach..

[6]

2.7.1 Particle colliders

If WIMPs are the DM, what can colliders tell us ? Given the energy of the LHC and the requirement that WIMPs have mass $\sim m_{weak}$ and interact through the weak force, WIMPs will almost certainly be produced at the LHC. Unfortunately, direct WIMP production of $\chi\chi$ pairs is invisible. The production channel at particle collider looks like SM + SM$\rightarrow$ DM + DM Fig. 2.4. However, such events are undetectable, but are expected to produce "mono-jet" or "mono-photon" where the jet 'j' or photon comes from initial state radiation and which can provide signatures of WIMPs [6].

Information on WIMPs can only be obtained indirectly from the signature of missing transferred energy and momentum. Although the observation of missing particles is consistent with the production of DM, it is far from compelling evidence. The discussions given in the remaining parts of this sub-section are based on [6]. Particle physics experiments at the LHC may stringently constrain cross sections involving

DM and related particles. The thermal relic density may be compared to the observed density of DM, and their consistency would give us confidence that DM is actually produced in this way and is made of the particles produced at the collider. So far important ranges of the parameter space has been explored by LHC which are in agreement with standard model expectations [57].

A future facility known as International Linear Collider (ILC) is expected to provide improved results on DM mass and relic density constraints. Several qualitative studies, such as given in [58],[59] and [60], have investigated the capacity of LHC to determine the ranges of the parameter space depending on various conceivable DM scenario. To this end, these studies have marked precisely the range of values for the cold DM relic abundance which is in agreement with the expected precision measurements for both experiments at the LHC and the ILC. This is given in Fig. 2.5, the WMAP satellite together with other cosmological observations (yellow shaded region) have constrained the DM relic density Ω_χ to a fractional uncertainty of ± 8 % . This uncertainty is expected to be narrowed down to ± 2 % by its successor, Planck (green shaded region). It is also shown that while the WMAP and Planck can constrain Ω_χ, they are insensitive to the DM mass m_χ ; however, collider experiments are keen to perform both. Moreover, precision studies at the LHC (cyan shaded region) are believed to determine so many of the super-symmetric model parameters that the neutralino mass can be determined to ± 5 GeV and the thermal relic density can be predicted to $\pm 20\%$.

Measurements at the ILC (blue shaded region) could improve these constraints on mass and relic density to $\pm$ 50 MeV and $\pm 3\%$, respectively. Not that, the search of both nature and properties of the DM, is believed to provide robust result when there is consistency between the particle physics predictions and the cosmological observations. This would provide compelling evidence that the particle produced at the LHC is indeed DM. The mass, spin, and many other properties of the DM will also be determined at the same time at the colliders. Thus, colliders may finally help solve the question of the microscopic identity of DM.

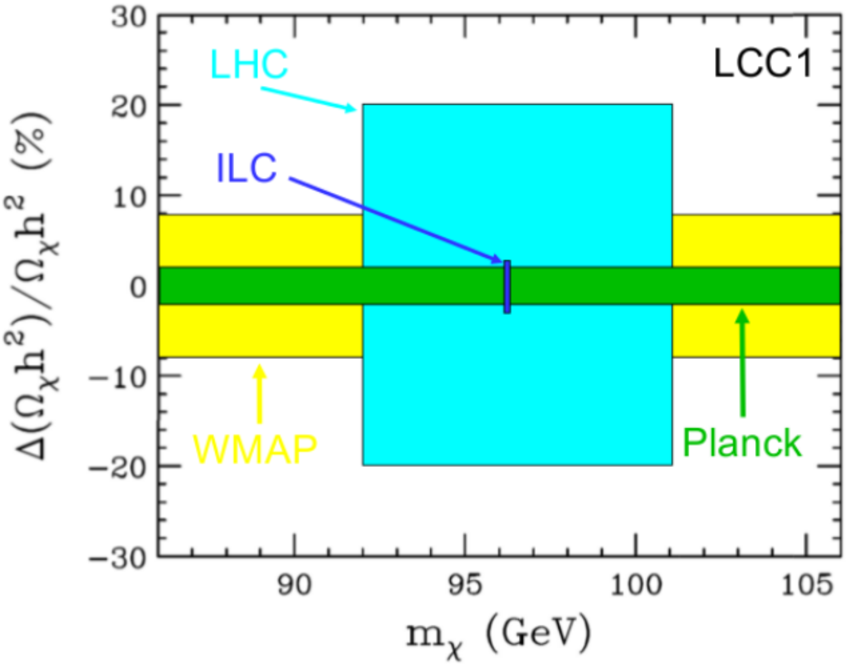

Figure 2.5: Constraints in the (m_χ , Ω_χ) plane from the LHC and the International Linear Collider, and from the WMAP [7] and WMAP and Planck measure Ω_χ , but are insensitive to the DM mass m_χ, the collider experiments bound both. These results are for LCC1, a supersymmetric model with minimal supergravity parameters Planck satellites

.

2.7.2 Direct detection strategies

Direct detection mechanisms of WIMPs involves an elastic scattering of WIMPs off normal matter through the interaction $DM + SM \rightarrow DM + SM$ as shown in the Fig.2.4 with an arrow pointing in the horizontal direction. This process is expected to deposit some recoil energy which may be detected. For example, considering parameters of weak interaction, i.e., taking the allowed WIMP mass between 10-1000 GeV the expected recoil energies induced by WIMPs will be in the range of 1-100 keV [61].

This will thus require a very sensitive detector placed deep in the ground to avoid contaminating radiations. The DM experiment which uses low-radioactivity sodium iodide crystals for example has observed a signal modulation. The solid red contours show the derived signal regions from DM experiment. If this is to be interpreted as a result of elastic scattering with WIMPs, it favors 10-15 GeV WIMPs if the scattering is from sodium, and 60-100 GeV for iodine [7]. Even though, the presence of various DM indications in the region around 10 GeV gave some excitement, improved results from several experiments indicate that probably in most cases, background was responsible for the observed events. This emphasizes the relevance of the background prediction and the quantification of its uncertainty. Overall, various direct detection experiments have been designed over the last decades. While there is no concrete evidence for DM detection, great progress has been achieved in direct DM searches . Moreover, it is expected that future experiments will increase the target masses to achieve an even higher sensitivity which will allow them perform a high statistics measurement of the DM particle properties.

2.7.3 Indirect detection strategies

Indirect DM detection try to detect self-annihilation products of DM particles in high DM density environments. DM cannot only be detected directly in dedicated experiments searching for nuclear recoils from the scattering of DM particles or produced in particle accelerators such as the LHC, but it can also reveal its existence indirectly. An indirect detection mechanism involves annihilation of WIMPs to produce SM particles. The process is indicated in Fig.(2.4) (i,e., DM + DM $\rightarrow$ SM + SM).

The total number of DM particles does not change significantly after "freez-out" in the early universe, but their spatial distribution changes considerably during structure formation. The very self-annihilation that plays a central role in this "freez-out" can give rise to a significant flux of gamma-rays, neutrinos, and even antimatter such as antiprotons and positrons, especially in regions with large DM density. The energy of the secondary particles can reach up to the mass of the DM particle, which typically would be a few hundred GeV. Since DM annihilation scales with the square of its density, indirect detection is more sensitive to cosmological and astrophysical processes than is direct detection [62].

Therefore, it is necessary to look for an observable consequences of DM in the emission of the DM annihilation products and their signals in objects of the cosmic structures such as halos of galaxies, dwarf galaxies and galaxy clusters which are characterized by their large DM densities. For example, dwarf spheroidal galaxies which are close satellites of the Galaxy are known for having a large value of mass-to-light ratio thus containing large portion of DM. They are also known for not showing intense star formation and non-thermal high-energy gamma-ray emission which make them a promising search sites for signals from DM annihilation process

[63]. While direct detection is the cleanest technique to unambiguously study the nature and composition of DM; it is also expected that some of the fundamental particles nature of DM can be probed with the detection of photons, neutrinos or charged cosmic rays that are produced by DM. These signals can be studied across gamma-ray spectrum [1], [64]. The spectrum will be found as combination of IC scattering, bremsstrahlung, and direct photon emission. And all of these emission forms are non- thermal as they depend on the energy distributions of the products of prompt WIMP.

2.8 Non-thermal processes in galaxy cluster

Galaxies in clusters also produce nonthermal emission in a variety of ways. AGN, which are often found in the central galaxies of relaxed clusters, are obvious examples of cosmic ray accelerators that produce a broad spectrum of nonthermal emission, from radio synchrotron emission up to emission in the gamma-ray band [65]. However, this type of emission from an AGN is clearly associated with the galaxy itself, and not with the separate population of cosmic rays that are distributed throughout the ICM [66].

Star formation is also tied to the production of nonthermal particles in galaxies. Supernovae, the final stage in the lifecycles of massive stars, are efficient particle accelerators of nuclei, protons, and electrons. Cosmic-ray electrons can synchrotron radiate, observable in the radio band, and IC scatter starlight up to gamma-ray energies. Cosmic-ray protons and nuclei can collide with interstellar matter to produce neutral pions that decay to gamma rays [67].

Radio and gamma-ray luminosities are tightly correlated with the star-formation rate in star forming galaxies [68]. In galaxy clusters, this correlation between star formation rate and gamma-ray luminosity can be used to set lower limits on the gamma-ray emission from clusters, by considering only the emission from star-forming galaxies [65].

2.9 The source of the relativistic particles and gamma-ray in galaxy cluster

It is fact that most of the cosmic rays produced in clusters of galaxies remain confined for a long time within the cluster potential wells and consequently produce high energy gamma-rays through their interactions with ICM. The emission of γ-rays from galaxy clusters is expected to be high, for example, due to IC Scattering and non-thermal bremsstrahlung by relativistic electrons [69]. Moreover relativistic protons, being the dominant non-thermal component of galaxy clusters, enhance the probability of hadronic interactions between thermal and non- thermal protons [70][71] that produce γ-ray emissions through the decay of pions and inject secondary particles.

The emission of γ-rays from galaxy clusters is also expected to be the result of the DM annihilation processes [72][73]. Although a γ-ray signal from the cluster volume is expected to arise through interactions of cosmic ray protons with the ambient plasma, currently there is no clear evidence for the detection of emissions in the γ-ray band in galaxy clusters [74], [75]. Therefore, this is suggestive of the presence of some problems with the current models or observations. Moreover, the recent derived Fermi-LAT upper limits on the content of cosmic rays [75] is a severe problem for all the known models [75], except possibly for the DM ones [76]. In addition to the optical, radio, and X-ray, and γ-ray bands, galaxy clusters are also expected to emit in the extreme ultraviolet, hard X-ray, and microwave frequencies.

2.10 The source of relativistic particles from galaxy cluster

2.10.1 Secondary electrons

Secondary electrons also called hadronic models that is one of models which suggest mechanisms for the origin of relativistic electrons in galaxy cluster. In this model relativistic electrons are believed to be produced as a result of interaction between non- thermal protons and the protons from the gas in the ICM [77][78] and [79]. The reactions that lead to the production of secondary electrons are described by the secondary electron model. There are different types and sites of particle acceleration in galaxy clusters from which gamma-rays and neutrinos can be produced through the following channels:

$p + p \longrightarrow \pi^{\pm} + \chi$

where χ represents any reachable final state from the initial state. The charged pions ($\pi^{\pm}$) the decay time and will decay into electrons, positrons and neutrinos via muons;

$\pi^{+} \longrightarrow \mu^{+} + \nu_{\mu}(2.6 \times 10^{-26} sec)$,

$\pi^{-} \longrightarrow \mu^{-} + \overline{\nu}_{\mu}(2.6 \times 10^{-26} sec)$,

and

$$\mu^{+} \longrightarrow e^{+} + \nu_{e} + \overline{\nu}_{\mu},$$

$$\mu^{-} \longrightarrow e^{-} + \overline{\nu}_{e} + \nu_{\mu} \tag{2.15}$$

, Similarly, the neutral pions (π^{0}) will decay predominantly into γ-rays and decay time:

$$p + p \longrightarrow \pi^{0} + \chi,$$

$$\pi^{0} \longrightarrow \gamma + \gamma(8.3 \times 10^{-17} sec) \tag{2.16}$$

In the pp collisions giving rise to γ-ray production, bullet protons are supplied by the previous particle accelerators found within galaxy clusters [7]. This model also predicts γ-rays from pion decay Eqn. (2.16) as well as neutrinos Eqn.(2.15), which can be tested with new generation γ-ray telescopes [80]. One of the problem of the secondary model include, the worst problem being the lack of gamma-ray detection [81].

2.10.2 Secondary electrons from DM annihilation process

Secondary electrons/positrons from DM annihilation process is the one of model that suggested as a possible source of relativistic particle in galaxy clusters. In this model DM annihilation/decay processes are believed to produce a wide range of standard particles and radiations such as electrons, positrons and gamma-ray radiations [7]. Electrons and positrons will undergo energy losses through their interactions with the particles in ICM and will emit in a gamma-ray spectrum after reaching equilibrium states through various emissions mechanisms [1].

These process of emission along with the standard formulas of the emissions from DM annihilation processes are given in Chapter 3. We have focus the discussion to more advanced problems which is addressed in this work, that is connected with the spatial distribution of the DM. As has been mentioned in Chapter 2, this work will focus upon one popular and most favored DM candidate called the neutralino. Neutralino is, a cold DM particle (as it moves with non-relativistic speed), and a member of a large group of DM particles, the WIMPs (see Section 2.4.3). Neutralino are also the lightest particle from the minimal super-symmetric extension of the standard model (MSSM) which are introduced by a minimal model of super-symmetry. According to this model particles occur in super-multiplets (also known as super-partners) which is often summarized as every boson is paired with a fermion and vice versa. The neutralino forms an attractive model because it is neutral, weakly interacting, and has viable mechanisms for the production of a thermal relic population [10].

Neutralinos are believed to annihilate into neutral pions which then decay into high-energy γ-rays. In addition to this their annihilation/decay processes are also believed to produce a wide range of standard particles such as electrons, positrons, that are formed either directly or from charged pion decay. Electrons and positrons will undergo energy losses through their interactions with the particles in ICM and in the highly magnetized environment of cosmic structure to emit in a multi-wavelength spectrum after reaching equilibrium states through various emissions mechanism [1].

These mechanisms which are neutral pion decay, IC scattering, and Bremsstrahlung radiation processes in γ-rays will be modeled in Chapter 3 using data from high-resolution cosmological simulations. Neutralino annihilation would thus result in non-thermal emissions, characteristic of the DM particle, from any structure that played host to a concentration of such particles. Additionally, the increasing sensitivity of astronomical measurements and the limitations of current ground-based direct detection experiments combine to elevate indirect detection methods (see Section 2.5.3) to new levels of competitiveness when it comes to setting limits on the nature of DM. Authors have studied the astrophysical consequences of these assumptions laid on secondary electrons from DM annihilation process such as [1] Moreover, today the construction of modern and sensitive instruments Cherenkov Telescope Array (CTA) in γ-ray bands have raised hope that detailed information regarding the spatial distribution of the emissions are achievable [7]. Motivated by these observations, in this thesis we have studied the effect of the realistic distribution of the DM in the simulated Coma like cluster on its emission in the gamma-ray bands. Thus, to address the above mentioned issues, we have take neutralino masses of 35 GeV with $b\bar{b}$ composition and DM annihilation cross-section of 3.0×10^{-26} cm^3 s^{-1} to produce the gamma-ray emission maps from DM annihilation processes. Based on a realistic modeling of the DM distribution using MUSIC-2 cosmological simulations data (see Section 3.3.2).

This results will also reflect how well the DM distributions are represented in the simulations through a simple semi-analytical DM model of the emission processes presented in Chapter 3. We have also demonstrate how the simulation of galaxy clusters and their DM content can be used to estimate the gamma-ray emissions from these objects. In this way, not only the expected γ-ray spectrum Fig.4.9a can be predicted but also the spatial distribution of the emissions Figs.4.4a and 4.4b. Moreover, comparison of the results we have followed to study the γ-ray band, following which gamma-ray emission will be studied as a more suggestive environment to obtain signals from the DM annihilation processes.

2.11 Summary

During the last 70 years, a new paradigm has emerged in which the matter visible to us in current telescopes only represents a small fraction of the total amount present in the Universe. Most of the matter instead appears to be in some form which is completely invisible, it does not emit, absorb or reflect light on any frequency. This is what is referred to as DM. The existence of matter in a large amount of non-baryonic, non-luminous matter component in the mass-energy budget of the universe is known as "DM". DM does not interact with the electromagnetic spectrum. However, its particle nature is still unknown thus remains to be one of the most significant problems of modern physics. Also, the current observational data give us very little information as to what form DM might take. A class of DM particles which are cold WIMPs are the most viable candidates among large number of proposed particle candidates for DM. This is because they have several important particle properties such as mass, stability (lifetime), scattering cross-section with nucleons, and cross-section for pair annihilation etc., which are both theoretically well motivated and begin to be constrained through various experiments. The final particle detail for WIMPs are obtained from the products into which they annihilate or decay. These particle properties will define whether or not we can observe WIMPs through their interaction with nucleons or their annihilation/decay into standard model particles. The secondary electrons as gamma-rays produced, which this thesis is based on, are believed to be produced from DM annihilation/decay processes. These electrons are also expected to undergo energy losses through their interactions with the particles in ICM and magnetic field thus undergo energy losses to provide an equilibrium spectra which will emit in a gamma-ray spectrum via various emissions mechanisms.

CHAPTER 3

Methodology and Data Presentation

3.1 Introduction

When two DM particles come close to each other, it is expected that they annihilate each other, producing standard model (SM) particles such as neutral and charged pions.
The neutral and charged pions will decay into gamma-rays and relativistic electrons /positrons, respectively in relatively short time. These secondary electrons/positrons will produce gamma-rays from Bremsstrahlung radiation and Inverse Compton Scattering (ICS) processes [82]. In this chapter, we present the mathematical models which are necessary to determine the local emissivity and ultimately the gamma-ray flux. In addition, data sources and data analysis are briefly described in the following presented are also briefly described sections.

3.2 Data presentation

In order to study the gamma-ray emission from DM annihilation process in galaxy clusters we have used the MUltidark SImulation of galaxy Clusters (MUSIC)-dataset as our first data source. MUSIC-dataset is a large subset of a mass limited sample of resimulated clusters selected from the MultiDark Simulation which is a DM only N-body simulation with 2048^3 particles in a 1 h^{-1} Gpc cubic box. This simulation run was done using the best-fit cosmological parameters to WMAP7 + BAO + SNI (Ω_M = 0.27, Ω_b = 0.0469, Ω_Λ = 0.73, σ_8 = 0.82, n = 0.95, h = 0.7). The MUSICs has a large numbers of samples (282 clusters and thousands of groups) and a high resolution [84]. The data in the MUSIC simulation contain the particle mass and coordinates divided into different mesh or grids (i.e, 21, 101, 201, 401, or 801). From this large number of samples avialable on the MUSIC-dataset we have taken three simulated Coma like galaxy clusters were taken namely, SGC280, SGC281 and SGC282 where the sample selection was done in order to optimize the resolution and computation time. Therefore, our samples SGC280, SGC281 and SGC282 were divided by 201 grids allowing us to obtain comparatively good resolution and low computation time.

The second data source that we have taken into account was the Dark Super Symetry (DarkSUSY) package. The DarkSUSY package is a fortran package that calculates the yield of different particles and radiations per neutralino annihilation. In this package the simulation is done for 8 "fundamental" annihilation channels $c\bar{c}$, $b\bar{b}$, $t\bar{t}$, $\tau^+\tau^-$, W^+W^-, Z^0Z^0, gg and $\mu^+\mu^-$ and different masses of neutralino [83]. A specific case we have taken as an initial spectra of electrons and gamma-rays per neutralino annihilation for a neutralino mass of 35 GeV dominated by a $b\bar{b}$ species.

3.3 Modeling the gamma-ray emission

Since gamma-ray emission is expected as a natural by-product of the self annihilation of super-symmetric DM particles, we have studied this emission in galaxy clusters by considering the annihilation of neutralino which is mainly composed of $b\bar{b}$ species. We also have considered a neutralino mass of 35 GeV, which has been tested in [7] to be a viable model for the production of secondary electron and radiation, with the annihilation rate of 1×10^{-26} cm^3 s^{-1} in three simulated Coma like galaxy clusters located at a redshift of z = 0.028. For the annihilation channel we have considered a branching ratio of 1.
In the following subsections we present the necessary mathematical expressions that helps us to model the gamma-ray emission from the annihilation process of WIMPs.

3.3.1 The equilibrium spectra of emitting particles

The relativistic electrons injected into the ICM are described by the quantity known as the source function or source spectra. The source spectra is the number of electrons and gamma-ray produced per unit time, energy and volume element at the position r from neutralino, χ, annihilation processes. It is given by the product of the neutralino pair number density N(r), neutralino annihilation rate <σV>, the production (initial) spectra $\frac{dN_i^f}{dE}$ and branching ratio B$_f$, i.e,

$$Q_i(E,r) =< \sigma V > \sum_f \frac{dN_i^f}{dE} B_f N_\chi(r), \tag{3.1}$$

where i and f refer to the produced particle and the kinematically allowed annihilation final states each with branching ratio of B_f, respectively. The neutralino pair number density N_χ(r) can be expressed as $\frac{\rho^2_{DM}}{2m^2_\chi}$, where the factor 2 in the denominator appears to take into account the annihilating pairs. The production spectra $\frac{dN^f_i}{dE}$ is obtained using DarkSUSY package [85].

The "electrons equilibrium spectra" can be obtained from the source spectra of the injected electrons by considering their energy loss by different mechanisms, and their spatial diffusion process as they pass through the atmosphere of the DM halo. The non-thermal electrons produced in the DM annihilation processes are subject to the effect of energy losses and spatial diffusion in the magnetized plasma of the cluster. This process is governed by the diffusion equation in the following form:

$$\frac{\partial}{\partial}\frac{dn_e}{dE} = \nabla\left(D(E,r)\right)\nabla\frac{dn_e}{dE} + \frac{\partial}{\partial E}\left(b(E,r)\frac{dn_e}{dE}\right) + Q_e(E,r), \tag{3.2}$$

where $\frac{dn_e}{dE}$ is the electron/positron spectrum, D(E,r) diffusion coefficient, b(E,r) the energy loss factor and Q_e(E,r) the electron "source spectra". A generic solution to the diffusion equation which in the case of galaxy clusters, where the effect of diffusion of electrons are negligible, is given by [86]. This solution which is the "electrons equilibrium spectra" has the form:

$$\frac{dn_e}{dE} = \frac{1}{b(E)}\int_E^{M_\chi} Q_e(E',r)dE', \tag{3.3}$$

where E is the energy of the electrons and b(E) (see Eq. 3.4) is the energy loss term in units of GeV s^{-1} which is the sum of effects due to ICS, synchrotron radiation, Coulomb losses and bremsstrahlung radiation [1].

$$\begin{aligned} b(E) &= b_{IC}E^2(1+z)^4 + b_{sync}E^2B^2 \\ &+ b_{Coul}n_e(1+z)^3\left(1+\frac{1}{75}\log\left(\frac{\gamma}{n_e(1+z)^3}\right)\right) \\ &+ b_{Brem}n_e(1+z)^3\left(\log\left(\frac{\gamma}{n_e(1+z)^3}\right)+0.36\right), \end{aligned} \tag{3.4}$$

where γ = E/m_e and b_{IC}, b_{synch}, b_{coul}, and b_{brem} are the Inverse Compton Scattering, synchrotron, Coulomb and Bremsstrahlung energy loss factors in units of GeV s^{-1}, respectively. **B** is a magnetic field defined from the gas distribution as in [7] and is given by: B(r) = B_0 (1 + $(r/r_s)^2)^{-q_b}$, where r_s and q_b are the scaling radius and exponent, respectively. The "electrons equilibrium spectra" can be used to calculate the local emissivities and ultimately the flux, which will be used in the following sections.

In the following subsections mathematical expression for the different gamma-ray emission mechanisms such as: neutral pion decay, ICS processes and non-thermal bremsstrahlung process are presented.

3.3.2 The gamma-ray flux from pion decay

When DM annihilation processes produce neutral pions, these unstable particles decay into gamma-rays whose spectrum obeys a power-law, i.e, they decay into less number of gamma-rays per energy of the photons at higher frequencies. The differential gamma-ray flux density from pion decay is then obtained by considering the annihilating DM pairs with mass M_χ, their velocity averaged annihilation cross-section $<\sigma V>$ and integrating over volume integral of the DM density ρ DM square along the line-of-sight divided by area. Hence, the differential flux which is number of gamma-ray photons per area per time and per energy at luminosity distance D_L is given by:

$$\frac{dF}{dE} = \frac{<\sigma\nu>}{2M_\chi^2}\frac{dN}{dE_\gamma}\int_0^r \frac{\rho_{DM}^2 dV}{4\pi D_L^2}, \tag{3.5}$$

where $\frac{dN}{dE_\gamma}$ is the initial gamma-ray spectrum which is obtained using DarkSUSY package [85]. The gamma-ray flux from pion decay can then be obtained by integrating Eqn.(3.5) over E_γ, the energy of gamma-ray photons producing the gamma-ray spectrum.

3.3.3 Gamma-ray emission from ICS processes

ICS processes involve the scattering of low energy photons to high energies by ultrarelativistic electrons so that the photons gain and the electrons lose energy. The process is called inverse, because the electrons lose energy rather than the photons, the opposite of the standard Compton effect. ICS of relativistic electrons and positrons on target cosmic microwave background (CMB) photons give rise to a spectrum of photons. Let $E = \gamma m_e c^2$ be the energy of electrons and positrons, ϵ that of the target photons and E_γ the energy of the scattered photon. The Inverse Compton power is obtained by folding the differential number density of target photons with the ICS cross section [1]. Relativistic electrons produced from charged pion from DM annihilation process scatter CMB photons and boost them to gamma-ray. The average IC power is given by

$$P_{IC}(E_\gamma,\gamma,r) = cE_\gamma\int_0^\infty d\epsilon n(\epsilon)\sigma(E_\gamma,\epsilon,\gamma), \tag{3.6}$$

where n(ϵ) is the blackbody spectrum of the CMB photons, and σ(E$_\gamma$,ϵ, γ) is the ICS cross-section given in [86] as

$$\sigma(E_\gamma, \epsilon, \gamma) = \frac{3\sigma_T}{4\epsilon\gamma_2} G(q, \Gamma_e), \tag{3.7}$$

where σ_T is the Thomson cross-section, γ is the electron Lorentz factor, and

$$G(q, \Gamma_e) = \left[2qlnq + (1 + 2q)(1 - 2q) + \frac{(\Gamma_e q)^2 (1 - q)}{2(1 + \Gamma_e q)} \right], \tag{3.8}$$

with

$$\Gamma_e = \frac{4\epsilon\gamma}{(mc^2)}, q = \frac{E_\gamma}{[\Gamma_e(\gamma mc^2 - E_\gamma)]}. \tag{3.9}$$

Folding the IC power with the spectral distribution of the equilibrium number density of electrons and positrons, we get the local emissivity of IC photons of energy E$_\gamma$. That means the local emissivity is obtained by integrating the product of ICS power P$_{IC}$(E$_\gamma$,γ,r) and electron equilibrium spectrum N$_e$(γ,r) across all electron energy as [1]

$$j_{IC}(E_\gamma, r) = \int_{\gamma min}^{\gamma max} N_e(\gamma, r) P_{IC}(E\gamma, \gamma, r). \tag{3.10}$$

The flux of gamma-rays from ICS process at luminosity distance D$_L$ can then be calculated by

$$S_{IC}(E_\gamma) = \int_0^r d^3 r' \frac{j_{IC}(E_\gamma, r)}{4\pi D_L^2}. \tag{3.11}$$

3.3.4 The gamma-ray emission from non-thermal Bremsstrahlung radiation

Bremsstrahlung or deceleration radiation (form German bremsen "to brake" and Strahlung "radiation") is a very important radiation mechanism in laboratory and astrophysical plasmas. Bremsstrahlung or free-free emission is often considered as a radiation of decelerating electron in the Coulomb field of an ion [1]. The last relevant contribution to the photon emission of galaxy cluster due to relativistic electron/positron is the process of non-thermal Bremsstrahlung, that means the emission of gamma-ray. The average power of non-thermal Bremsstrahlung emission is calculated by considering the number density of ions n$_j$(r)

$$P_B(E_\gamma, \gamma, r) = cE_\gamma \sum n_j(r) \sigma_j(E_\gamma, E), \tag{3.12}$$

with the sum including all species j in the intra-cluster medium (ICM), each with number density n$_j$ (r). Where the interaction cross-section is give in [86]

$$\sigma(E_\gamma, E) = \frac{3}{8\pi} \sigma\alpha T \left\{ \left[1 + \left(1 - \frac{E_\gamma}{E}\right)^2 \right] \phi_1 - \frac{2}{3}\left(1 - \frac{E_\gamma}{E}\right) \phi_2 \right\}, \tag{3.13}$$

with

$$\phi_U = 4\left\{ln\left[\frac{2E}{mc^2}\left(\frac{E-E\gamma}{E\gamma}\right)\right]-\frac{1}{2}\right\}.$$

The local emissivity can be obtained by integrating the product of non-thermal Bremsstrahlung power $P_B(E\gamma,\gamma,r)$ and electron equilibrium spectrum $N_e(\gamma,r)$ across all electron energy as

$$j_B(E\gamma, r) = \int_{\gamma min}^{\gamma max} d\gamma N_e(\gamma, r) P_B(E\gamma, \gamma, r). \tag{3.14}$$

The gamma-ray flux from non-thermal Bremsstrahlung processes at luminosity distance D_L is determined in a similar fashion to the above emission mechanisms by using the local emissivity as in

$$S_B(E\gamma) = \int_0^r \frac{d^3r' j_B(E\gamma, r')}{4\pi D_L^2} \tag{3.15}$$

Eqn. (3.15) has been used to determine the differential gamma-ray flux.

3.4 Data analysis

The raw data we have taken from the MUSIC simulation contains DM particle coordinates and masses of three simulated Coma like galaxy clusters (i.e, SGC280, SGC281 and SGC282). From this raw data for the position and mass of DM particle, we used SPH-kernel to determine the density of DM on a grid based on Eq. (3.16) below.

$$\rho_{on\ a\ grid}(r) = \sum_i m_i W(r - r_i, h), \tag{3.16}$$

where $\rho_{on\ a\ grid}$ is the particle density on a grid of size (10 kpc)^3, m_i is the mass of particles (in our case neutralino and gas), the scaling factor $W(r-r_i, h)$ is called the kernel, and h describes the characterstic width of the kernel which is normilized to unity [87].

Next to this important procedures, we used a fortran code to allocate the DM and gas density on a three dimensional cube of side 2 Mpc which is grided into smaller cubes of side $\sim$ 10 kpc (the simulated galaxy clusters which are (2 Mpc)^3 in volume are divided into $\sim$ 8 millon small cubes of side $\sim$ 10 kpc making 201 grids on each sides of the clusters. Thus, for one side of the clusters the grids give about 40,401 square boxes). Now knowing the DM and gas density in each cube help us to determine and allocate the magnetic field and electron density within the cluster. Combining this results with the electron production spectra from the DarkSUSY package (a fortran package that calculate the yield of particles and radiations per a neutralino annihilation and our second data source) enables us to calculate all the necessary ingrediants for the gamma-ray emission i.e, the electron source factor Q_e (E,r), the electron equilibrium spectra $\frac{dn_e}{dE}$ and the average power radiated P(ν, E, r, z). Finally, the local emissivity is calculated and then the differential gamma-ray flux density from each mechanisms are computed in each cube based on Eqns. (3.5), (3.11) and (3.15). In addition to the fortran-95 program we have also used a python code to produce all our maps.

3.5 Summary

In this chapter we have described the mathematical modeling for all the quantities that are necessary to accomplish our objectives. We have specified a DM candidate for our work and also have presented all the mathematical models necessary to compute the gamma-ray flux from the annihilation process. The gamma-ray flux which are determined will then provide vital information for an indirect detection of DM through their annihilation process, as they can be detected using sensitive telescopes tuned in the appropriate frequency range. The data for the simulated Coma like galaxy clusters (i.e, SGC280, SGC281 and SGC282) of our interest are found available in the MUSIC-dataset and the DarkSUSY package is our source for the initial electron and gamma-ray spectra of a neutralino mass M_χ = 35 GeV.

CHAPTER 4

Result And Discussion

4.1 Introduction

For the purpose of studying the gamma-ray emission from the Coma cluster; DM annihilation/decay processes as the sources of relativistic electrons and radiations using mathematical models discussed in Sec. 3.3 to compute this emission have been applied on three simulated Coma like galaxy clusters. Following these, in this Chapter, we have presented the results obtained from the study of the gamma-ray emission of the simulated Coma like galaxy clusters in different forms (i.e, maps, graphs and tables) are presented. In the first section the DM distribution and the density maps for the clusters is presented. Then the gamma-ray flux and the emission maps at different photon energies are discussed. Finally, the differential gamma-ray flux densities obtained by the different mechanisms is presented accordingly.

4.2 Distribution of DM within the galaxy clusters

Evaluation of DM annihilation flux from neutralino χ involves a product of two terms: the term A_{DM}, the particle physics part, that depends on the particle physics model of DM, and the cosmological part which involves a line-of-sight volume integral of the square of DM density evaluated in each cube as given below [7][10]

$$\Phi = A_{DM} \int_{l.o.s} \rho_{\chi}^{2} dV, \quad (4.1)$$

where ρ_{χ} is the neutralino DM density. Taking the DM particle is determined information at redshift of zero, we determine the density ρ_i of the i^{th} DM particle using Smoothed Particle Hydrodynamics (SPH) kernel, which evaluates the density in a regular grid taking into account the 44 neighboring particles that gives high resolution in the simulation by considering line-of-sight in the cubic box Eqn. 4.1 [87]. This allows to easily compute the square of the DM densities integrated in the line-of-sight. In Figs. 4.1a and 4.1b we plot the projected map of the square of DM density values of a clusters 2 Mpc across that are obtained using SPH kernel and for each grid $\sim$ 10 kpc.

The brightest colors in the map clearly show enhanced DM density substructures which are required to correctly determine emissions from DM annihilation process in clusters. Becuase, annihilation rate for gamma-ray have been searched for in regions where the dark matter density is expected to be high as annihilation rate is proportional to the DM density squared ρ^2_{DM}. The DM density maps indicate how the DM density decreases as we move from the center to the edge of the clusters except at the substructures which are found off-center. We have observed that SGC281 has more number of emission in the center than SGC282 but on the other hand SGC282 has relatively dominant in all substructure of cluster than SGC281. When we observed the density maps in generally SGC282 is denser than SGC281. Since we have consider equal volume of clusters is considered the result describes as the implication that SGC282 have high mass in the given position of DM density.

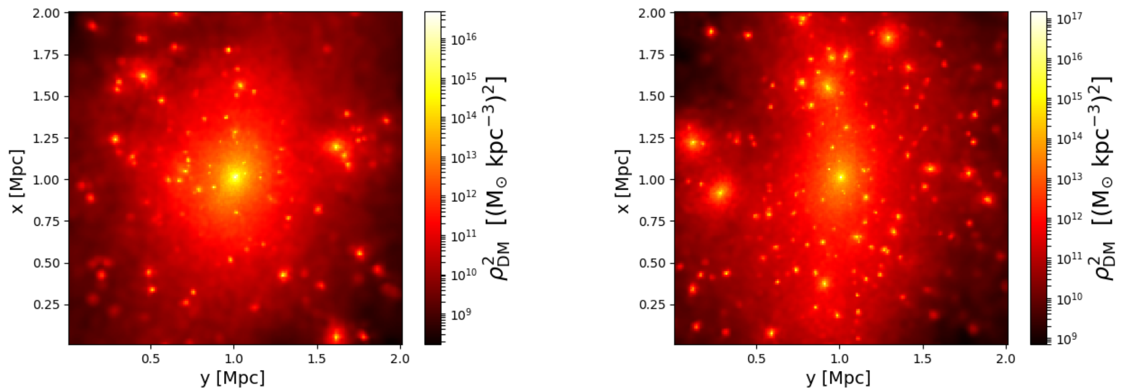

(a) **(b)**

Figure 4.1: The DM density square map of Galaxy Cluster (SGC281) and Galaxy Cluster (SGC282) in Fig a and b respectively are obtained using SPH kernel.

4.3 Density profile of one specific cluster

In order to determine DM annihilation flux from neutralino χ:- we have used MUSIC-2 simulation [88], which is a high resolution hydrodynamical, zoomed in simulation of 282 galaxy clusters. Fig. (4.2) shows the density profile of one specific cluster. The density profiles for DM, gas and stars, are given in red (solid curve), green (dotted curve) and blue (dot dashed curve), respectively. We compute the densities in terms of their mean density which will allow us to compare between the three species.

At the outskirts of the cluster the slope of the DM and gas density profiles are very

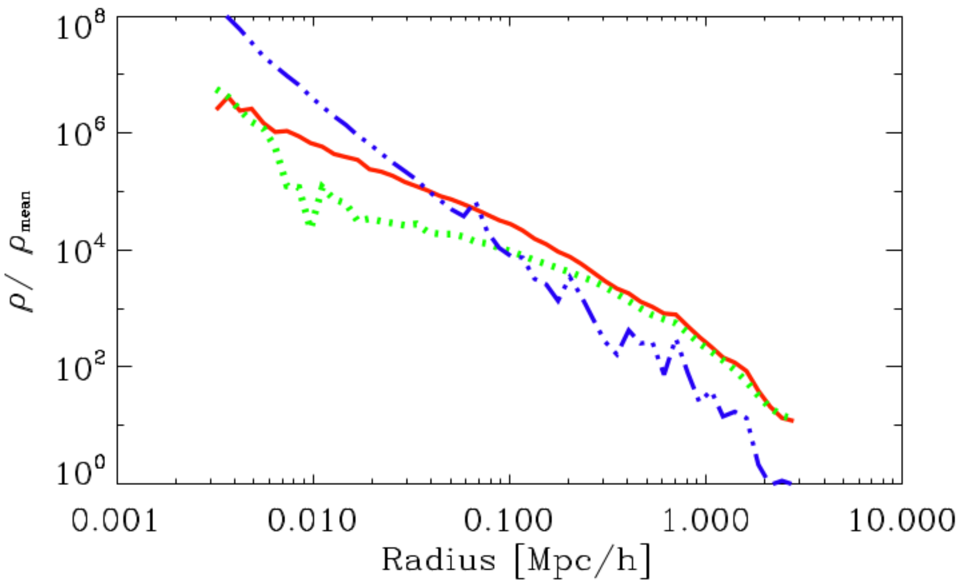

Figure 4.2: The density profile of DM, gas and stars in red solid , green dotted and bluedot dashed curve, respectively [7]

.

similar and stays above that of the stars, which is expected as the number of stars should decrease in the outer region (less galaxies). On the other hand, we observe that a gradual increase in the number density of the stars becuase the densities in terms of their mean density of the baryonic matter have high mean density than non-baryonic matter for this reason the number density of stars increase. In fact in the cluster baryonic matters (stars and gas) and non-baryonic matter (DM) so, we considering their densities in terms of their mean density of baryonic matters and non-baryonic matter for our comparession. Almost each peak in the dot dashed line represents an encounter of a new galaxy, towards the inner region as most of the baryonic mass is going into forming the stars. The fact that the stars are the dominant component in the inner region of the cluster is a manifestation of the over cooling problem, a well known feature in current cosmic simulations due to shortcomings in the prescription of feedback mechanisms.

4.4 The distribution of DM in different galaxy clusters

The DM density distribution for the three galaxy clusters SGC280, SGC281 and SGC282 are presented in Fig.4.3. Comparatively the DM density distribution of the three galaxy clusters, this SGC282 have relatively densiest DM distribution at all points while radius increases. In the radial distribution of the DM SGC280 and SGC281 have radially similar DM distribution at point radius 0.04 Mpc and solar mass of 4×10^{9} kpc^{-3}. But above the given point DM density distribution is denser in SGC281 than SGC280 and at the edge they have approximately the same. In Figs.4.1a and 4.1b and 4.3 inorder to detect the DM or to know from which regions of the galaxy cluster the higher emission coming from had been consirdered. In fact higher emissions were originated from the regions where the annihilation rate which is proportional to the square of the DM density square. Therefore, all the densest regions on the maps which are near to the center and away from the center the source of higher gamma-ray emission and the expected gamma-ray emission can be emanate from centeral part of galaxy cluster.

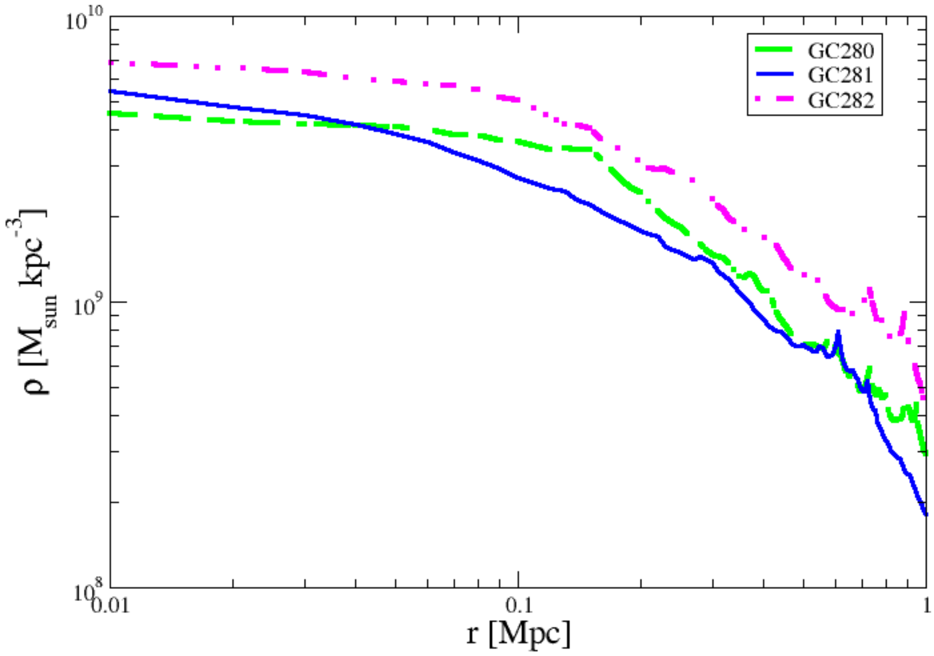

Figure 4.3: Comparision of DM densities binned on log-scale r from three galaxy clusters

.

4.5 Gamma-ray flux and emission maps

Gamma-ray emission maps have been produced by using all important processes in (see Section 3.3.2). We choose neutralino mass M_χ = 35 GeV have been choosen and composition of $b\bar{b}$ which is the best fitting DM species and mass for DM annihilation models has also been suggested by the data of Cosmic Ray (CR) antiproton spectrum obtained by PAMELA [89] which is in agreement with the result of [90].

In Figs. 4.4a and 4.4b we have provide the results obtained along with their discussion. The gamma-ray emission maps obtained from neutral pion decay processes at a photon energy of 9 MeV is shown in Fig. 4.4a. The magnitude of the differential gamma-ray flux of the neutral pion decay is 9×10^{-13} ph. cm^{-2} s^{-1}GeV^{-1} ; this value is 8 times larger than that of non-thermal Bremsstrahlung gamma-ray flux

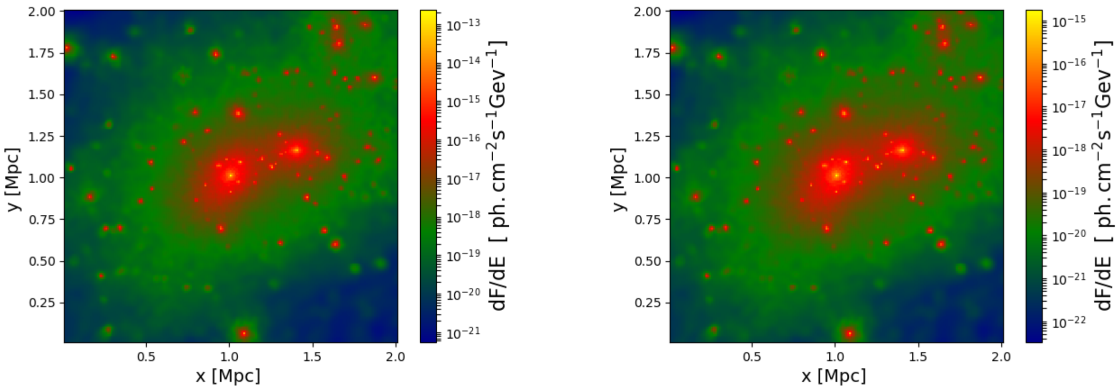

(a) (b)

Figure 4.4: Gamma-ray emission map from pion decay and non-thermal Bremsstralung for SGC280 at 9 MeV in a and b, respectively.

value for similar photon energy. It is possible to mention that the expected gamma-ray emission is related to differential gamma-ray flux. The map also indicates the gamma-ray emissions mostly coming from relatively denser region and it decreases the edge of substracture. The bright yellow color discribes the gamma-ray emission high in the center of the sub-halos; because the DM annihilation rate is high at the centeral region .

We can observe from Figs.4.5a and 4.5b the energy dependence of the gamma-ray emission from the gamma-ray flux obtained at 1 MeV the photon energy have the magnitude of the differential gamma-ray flux is $\sim$ 270 ph. cm^{-2} s^{-1}GeV^{-1} less than that of 100 MeV.

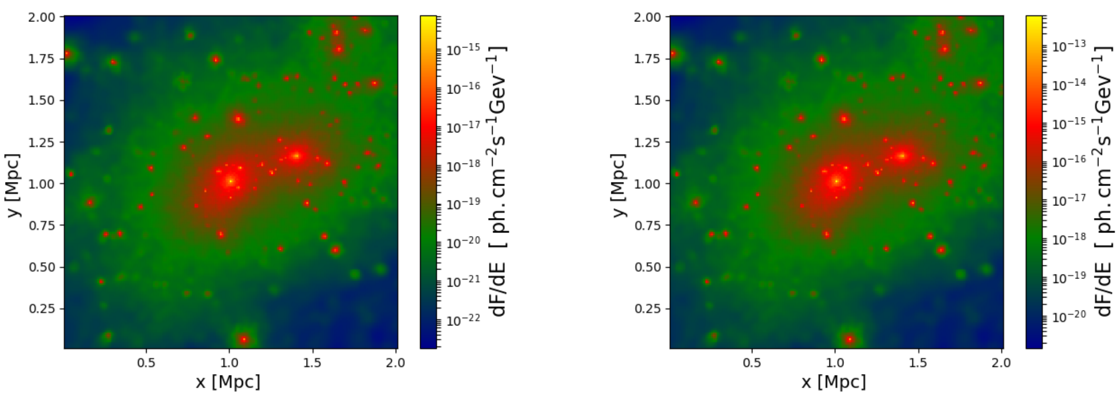

(a) (b)

Figure 4.5: Gamma-ray from pion decay processes at 1 MeV and 100 MeV for SGC280 in Fig a and b.

In all presented gamma-ray emission maps the gamma-ray emission mostly coming from relatively denser sub-hole to the edge of sub-structure and the gamma-ray emission in three cases; the gamma-ray emission produced in neutral pion decay map is in the process of DM annihilation of the neutral pion (unstable particles) decay in to the gamma-ray emission. On the other hand non-thermal bremsstrahlung and ICS we consider the relativistic electrons and positrons on the target of CMB photons give rise to the gamma-ray spectrum and the emission of photons in the defflection of charged particles by the electrostatic field of ion in ISM respectively. We have computed the gamma-ray emission from the differential gamma-ray flux (see Eqn.(3.5)) for different gamma-ray energy. Using the computed gamma-ray flux data from simulation we are able to produce a good resolution maps that allow us to look for possible structures and substructers distributed in the cluster regions. In Figs. 4.6a and 4.6b the gamma-ray emission for SGC281 and SGC282 presented at 100 MeV gamma-ray energy.

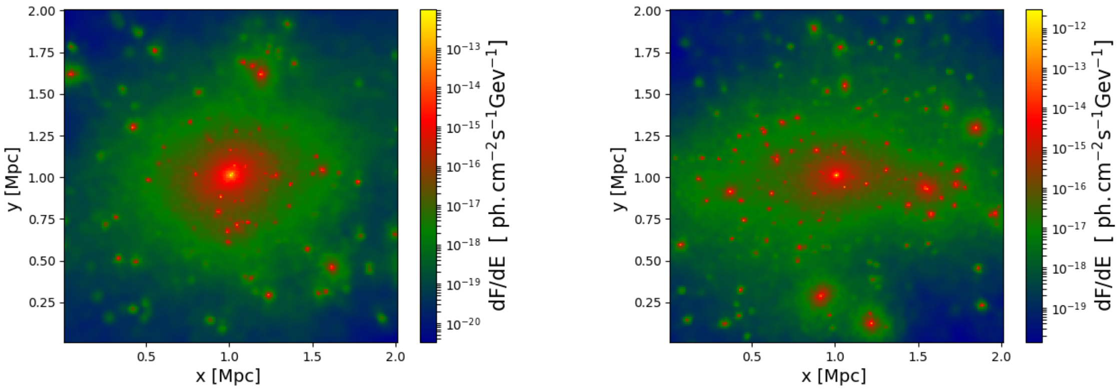

(a) (b)

Figure 4.6: Gamma-ray emission from pion decay processes at 100 MeV for SGC281 and SGC282 in Figs. 4.5 a and b, respectively.

In the gamma-ray emission maps we use the point to point comparation SGC282 is 3 times higher differential gamma-ray flux than SGC281. This is due to SGC282 have high DM mass expected than SGC281. Therefore, SGC282 have high gamma-ray emission centeral region to substructure than SGC281. But morphologically there is no significant difference among them. In generally we have to consider that without any confusion one can simply understand the similarity of Figs.4.4a, 4.4b and 4.5a,4.5b with the density square maps Figs.4.1a and 4.1b and the maps indicated that the higher emissions originated from the densest region of DM distribution or high annihiation rate and lower emissions from the less dense regions of DM distribution it has been prediction. In the SGC281 and SGC282 clusters gamma-ray emission maps the centeral regions and the sustructures found off-center are also clearly visible from the maps for both clusters.

4.6 Differential gamma-ray flux density

In the case of neutral pion decay for the three galaxy clusters SGC280, SGC281 and SGC282 the differential gamma-ray flux densities have ploted in (Fig. (4.7)). In the galaxy cluster SGC280 and SGC281 have slightly similar curve in the graph. This means the differential gamma-ray flux densities is approximately the same.

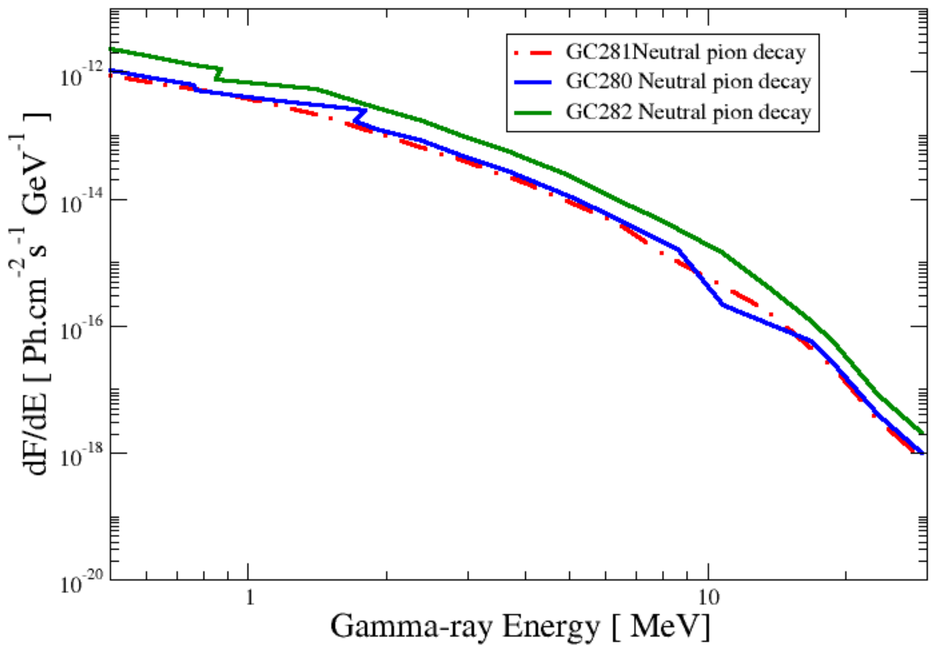

Figure 4.7: Differential gamma-ray flux densities from neutral pion decay in the three galaxy clusters SGC280, SGC281 and SGC282 with blue, red dot dashed and green curve, respectively

.

In the lower gamma-ray energy and the high gamma-ray energy, for ever they have a significant difference. At low gamma-ray energy SGC280 is 3 times high in differential gamma-ray flux than SGC281. On the other hand SGC282 is the dominant differential gamma-ray flux densities than SGC280 and SGC281 in the lower gamma-ray energy and high photon energy. Differential gamma-ray flux from neutra pion decay and non-thermal bremsstrahlung in the case of SGC280, SGC281 and SGC282 (see Fig.4.7). We presented this maps to see the differential gamma-ray flux densities in the case of non-thermal Bremsstrahlung has also similar manner to (Fig.4.8).

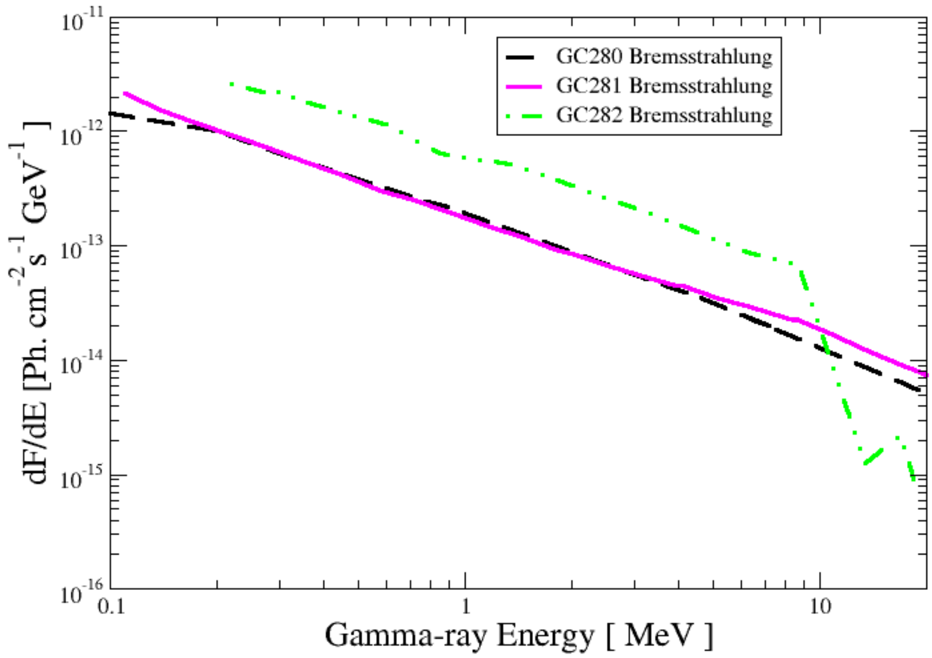

Figure 4.8: Differential gamma-ray flux densities from neutral pion decay and non-thermal Bremsstrahlung in three galaxy clusters SGC280, SGC281 and SGC282 with black, magneta and green dot dashed curve, respectively

.

For SGC280 and SGC282 have apprximatey same differential gamma-ray flux at gamma-ray energy 10.4 MeV and 1.2×10^{-14} ph. cm^{-2}s^{-1} GeV^{-1} differential gamma-ray flux but dominets above the specifyied points. Similarly SGC281 and SGC282 have also the same ditribution at the gamma-ray energy 9.8 MeV and 2.02×10^{-14} ph.cm^{-2}s^{-1} GeV^{-1} differential gamma-ray flux. On the other hand side SGC280 and SGC281 have similar dark matter distribution at gamma-ray energy between 0.1-4 MeV and 4×10^{-14} ph. cm^{-2}s^{-1} GeV^{-1} to 1.5×10^{-14} ph. cm^{-2}s^{-1} GeV^{-1}. Differential gamma-ray flux densities depend on the gamma-ray energy and its the galaxy cluster mass. We have ploted the differential gamma-ray flux densities obtained from pion decay and non-thermal Bremsstrahlung indicated in red and blue colors, respectively (Fig. 4.9a). The gamma-ray energy range on the x-axis starts at mass of electron 0.511 MeV to a complete annihilation/decay of neutralino mass of 35 GeV used.

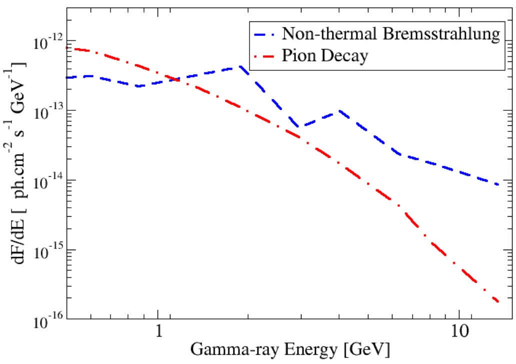

(a)

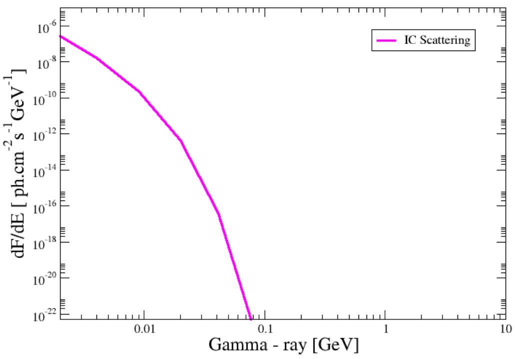

(b)

Figure 4.9: Differential gamma-ray flux densities from pion decay, non-thermal Bremsstrahlung and IC scattering processes for SGC280 is given in the plot with red dot dashed, blue dashed and pink solid curve, respectively.

For both non-thermal Bremsstrahlung and pion decay have the same photon energy at 1.4 GeV and have the same the differential gamma-ray flux at 2.7×10^{-13} ph. cm^{-2} s $^{-1}$ GeV^{-1} points and above 1.4 GeV photon energy the neutral pion decay is dominant and below the given photon energy non-thermal Bremsstrahlung is dominant. At 29 GeV non-thermal Bremsstrahlung and pion decay takes over until it decays completely at the mass of neutralino 35 GeV. The shape of spectra obtained here for neutralino mass of 35 GeV and composition $b\bar{b}$ is in agreement with the recent work in reference [7], [73] of a similar (intermediate range) neutralino mass of 43 GeV composition $b\bar{b}$. In the Figs. 4.9a and 4.9b the differential gamma-ray flux densities from the neutral pion decay, non-thermal Bremsstrahlung and IC scattering process in the given graph with red, blue and pink colors respectively are ploted by using the neutralino mass 35 Gev and the $b\bar{b}$ composion for the same photon energy but different gamma-ray flux for each cases and for each photon energy.

When we see the pion-decay graph the gamma-ray emission produced from the neutral pion (unstable particles) decay into gamma-ray. In the case of pion decay, it is dominant in higher photon energy because the neutral pion decay in to the less number of gamma-ray per energy of photon at higher frequencies, i.e frequence and pothon energy are proportianal and at low energy the gamma-ray flux is high. In Fig. 4.9b the IC scattering high at the low photon energy and IC scattering cases the gamma-ray emission produced by the relativistic electrons produced from the charged pion in the dark matter annihilation process and relativistic electron intract with CMB photons scatter and boosts the gamma-ray.

In the IC scattering at high photon energy have low differential gamma-ray flux this is because of at high electron energy in a short period of time the relativitic electrons interacted with CMB increases a few gamma-ray emission on that region. On the other side the low electron energy the relativistic electronos interact with CMB and produces high gamma-ray emission in along period of time. In Fig. (4.9a) when we compare non-thermal bremsstrahlung with the others neutral pion decay and IC scattering the differential gamma-ray flux density is intermediate range.

Pion decay and non-thermal Bremsstrahlung with the photon energy and the differential gamma-ray flux for the three galaxy clusters that presented in the table 4.1. To make the detaile comparision for the three galaxy clusters, we consider photon energy and differential gamma-ray flux. For the three free SGCs the photon energy increasing from zero to 35 MeV the differential gamma-ray flux decreases and approching to zero. That means the neutralino mass can be decayed and we cannot be detected the gamma-ray emission above this range. We consider for the same SGC and the same photon energy they have different differential gamma-ray flux and different for neutral pion decay and non-thermal Bremsstrahlung. This happens for free SGC280, SGC281 and SGC282, this can be summarized in the table.

Galaxy cluster	Pion decay		Bremsstrahlung	
	Photon energy(MeV)	Differential gamma ray flux(ph. $cm^{-3}s^{-1}GeV^{-1}$)	Photon energy(MeV)	Differential gamma ray flux(ph. $cm^{-3}s^{-1}GeV^{-1}$)
280	1	2.7 x 10^{-14}	1	1.9 x 10^{-10}
	29	2.0 x 10^{-18}	29	9.1 x 10^{-14}
	35	0	35	0
281	0.5	7.3 x 10^{-15}	0.5	2.2 x 10^{-12}
	29	9.8 x 10^{-19}	29	4.4 x 10^{-15}
	35	0	35	0
282	0.5	1.4 x 10^{-14}	0.5	2.2 x 10^{-13}
	29	2.1 x 10^{-18}	29	1.1 x 10^{-14}
	35	0	35	0

Table 4.1: Pion decay and non-thermal Bremsstrahlung for the minimum and maximum photon energy and differential gamma-flux for three galaxy clusters SGC280, SGC281 and SGC282.

4.7 Summary

In this chapter we summqrized the results obtained from the DM annihi- lation of neutralino for the simulated coma like galaxy clusters using the data from the MUSIC-dataset. Based on the DM annihilation process, in the case of neutralino mass of 35 GeV. The results help to produce a good resolution gamma-ray emission maps that shows for possible structures and substructures distributed in the cluster region which are required to obtain the expected gamma-ray emission from DM annihilation process. Gamma-ray emission maps and the DM density square maps were found to be identicaly providing the fact that higher emission originate from the densiest structure.

Presented maps in the all mechanism produced the gamma-ray emission is high at centeral structure. Where the DM content is relatively high and its annihilation rate is also high. It is possible to say the photon energy is depends on the differential gamma-ray flux. On the observational side, the independent experiments (both laboratory and astrophysical) devoted to constrain the nature and the properties of DM are important to understand the role of DM in the production of non-thermal emission in galaxy clusters. Regarding the possibility to obtain this information by direct observations of galaxy clusters, we point out that the best spectral bands to test these model is the gamma-ray bands.

CHAPTER 5

Conclusion

Most matter in the Universe is in the form of non-luminous DM and the particle nature of DM is still unknown. DM self-annihilation would provide a mechanism for an indirect detection of the DM particles [1]. We determine the gamma-ray emissions from neutralino DM annihilation processes considering neutralino masses, M = 35 GeV. The spectral features of the emission are expected to be closely related to the nature, composition of a DM particle [91][88].

We develop semi-analytical models which provide gamma-ray emission maps from DM annihilation processes in galaxy clusters. The high resolution and number of MUSIC clusters allows us to single out DM content, where it can be expected that the DM annihilation signal exceeds ordinary emission. Applying a SPH kernel allows us to determine the DM density at arbitrary locations within the cluster volume which is used to focus on the contribution of the gamma-ray emission maps of clusters. We have investigated DM indirectly by studying the gamma-ray emission from their annihilation processes in simulated Coma like galaxy clusters. We computed the gamma-ray emission from the neutralino DM annihilation considering for the given a neutralino mass, in three simulated Coma like galaxy clusters whose raw datas for the particle mass and coordinate are taken from the MUSIC-dataset. Using the photon energy results we are able to produce a good resolution maps of the gamma-ray emission that allow us to look for possible structures and substructures distributed in the cluster regions.

No significant morphological differences were observed between the maps at different photon energy and the gamma-ray emission maps are found to be similar to the DM density maps indicating that higher emissions emanated from the densest regions. In the cases of neutral pion decay, non-thermal Bremsstrahlung and IC scattering the produced maps giving the information about the gamma-ray emission comes from more DM denser region and which decreases at the edge of

the cluster. This is becuase the DM annihilation rate is higher in the centeral region as expected on averge. Relatively the DM density square is high and the gamma-ray emission is also greater. Among the three simulated galaxy clusters, simulated galaxy cluster SGC282 showes the densest DM distribution almost in all the regions of the map. The differential gamma-ray flux obtained from neutral pion decay process is on average an order of magnitude higher than that from non-thermal Bremsstrahlung process, for similar photon energy, for all the three simulated galaxy clusters. For all the three gamma-ray emission mechanisims from DM annihilation process, simulated galaxy cluster SGC282 showes dominant differential gamma-ray flux densities. Overall we have observed that the gamma-ray emission flux calculated in these simulated galaxy cluster from the DM annihilation process is higher from regions of denser DM halos in the simulated Coma like galaxy cluster as expected. We produced the gamma-ray emission map by using different simulation mechanism for different cases. In our observation pion decay is dominant in high photon energise and the IC scattering is in reverse case.
Since galaxy clusters are dominated by DM, consequently it is appropriate to consider the secondary electrons from DM annihilation processes as a model for the source of the relativi- stic electrons which are responsible for the gamma-ray emission in galaxy clusters. This opens the opportunity to extend this study using different annihilation channels and mass of neutralino to come up to compare the expected previous study of gamma-ray emission and spectrum of Coma cluster in the future.

Bibliography

[1] Sergio Colafrancesco, Stefano Profumo, and Piero Ullio. Multi-frequency analysis of neutralino dark matter annihilations in the coma cluster. *Astronomy & Astrophysics*, 455(1):21–43, 2006.

[2] DP Roy. Basic constituents of the visible and invisible matterâĂŤa microscopic view of the universe. 2000.

[3] Tjeerd S van Albada, K Begeman, R Sanscisi, and JN Bahcall. Distribution of dark matter in the spiral galaxy ngc 3198. In *Dark Matter in the Universe*, pages 7–23. World Scientific, 2004.

[4] Douglas Clowe, Maruša Bradač, Anthony H Gonzalez, Maxim Markevitch, Scott W Randall, Christine Jones, and Dennis Zaritsky. A direct empirical proof of the existence of dark matter. *The Astrophysical Journal Letters*, 648(2):L109, 2006.

[5] M Watanabe, K Yamashita, A Furuzawa, H Kunieda, Y Tawara, and H Honda. Temperature map of the coma cluster of galaxies. *The Astrophysical Journal*, 527(1):80, 1999.

[6] Jessica Goodman, Masahiro Ibe, Arvind Rajaraman, William Shepherd, Tim MP Tait, and Hai-Bo Yu. Constraints on dark matter from colliders. *Physical Review D*, 82(11):116010, 2010.

[7] Remudin Reshid Mekuria, Paolo Marchegiani, Andreas Faltenbacher, and Sergio Colafrancesco. Multi-wavelength emissions from dark matter annihilation processes in galaxy clusters using cosmological simulations. *PoS*, page 009, 2017.

[8] Gaëlle Giesen, Mathieu Boudaud, Yoann Genolini, Vivian Poulin, Marco Cirelli, Pierre Salati, and Pasquale D Serpico. Ams-02 antiprotons, at

last! secondary astrophysical component and immediate implications for dark matter. *Journal of Cosmology and Astroparticle Physics*, 2015(09):023, 2015.

[9] ShinâĂŹichiro Ando and Eiichiro Komatsu. Anisotropy of the cosmic gamma-ray background from dark matter annihilation. *Physical Review D*, 73(2):023521, 2006.

[10] Gerard Jungman, Marc Kamionkowski, and Kim Griest. Supersymmetric dark matter. *Physics Reports*, 267(5-6):195–373, 1996.

[11] Erik Zackrisson and Teresa Riehm. High-redshift microlensing and the spatial distribution of dark matter in the form of machos. *Astronomy & Astrophysics*, 475(2):453–465, 2007.

[12] Fritz Zwicky. Die rotverschiebung von extragalaktischen nebeln. *Helvetica Physica Acta*, 6:110–127, 1933.

[13] Denise Hurley-Keller, Mario Mateo, and Eva K Grebel. A new culprit in the second-parameter problem in the sculptor dwarf spheroidal galaxy? *The Astrophysical Journal Letters*, 523(1):L25, 1999.

[14] Margaret J Geller, Antonaldo Diaferio, and Michael J Kurtz. The mass profile of the coma galaxy cluster. *The Astrophysical Journal Letters*, 517(1):L23, 1999.

[15] Sinclair Smith. The mass of the virgo cluster. *The Astrophysical Journal*, 83:23, 1936.

[16] Masataka Fukugita and P James E Peebles. The cosmic energy inventory. *The Astrophysical Journal*, 616(2):643, 2004.

[17] Anna Kathinka Dalland Evans. *Mapping Dark Matter and Dark Energy*. PhD thesis, University of Oslo Oslo, Norway, 2009.

[18] Peter Ulmschneider. Vom urknall zum modernen menschen. 2014.

[19] Hans Volker Klapdor-Kleingrothaus and Y Ramachers. Dark matter in astro and particle physics. In *Dark matter in astro-and particle physics*, volume 1. Springer, 1997.

[20] Robert H Sanders. *The dark matter problem: a historical perspective*. Cambridge University Press, 2010.

[21] Alexey Vikhlinin, L VanSpeybroeck, M Markevitch, WR Forman, and L Grego. Evolution of the cluster x-ray scaling relations since z> 0.4. *The Astrophysical Journal Letters*, 578(2):L107, 2002.

[22] Maxim Markevitch. Chandra observation of the most interesting cluster in the universe. *arXiv preprint astro-ph/0511345*, 2005.

[23] Jan Tauber, PAR Ade, N Aghanim, MIR Alves, C Armitage-Caplan, M Arnaud, M Ashdown, F Atrio-Barandela, J Aumont, H Aussel, et al. Planck 2013 results. i. overview of products and scientific results. 2014.

[24] David N Spergel, Licia Verde, Hiranya V Peiris, E Komatsu, MR Nolta, CL Bennett, M Halpern, G Hinshaw, N Jarosik, A Kogut, et al. First-year wilkinson microwave anisotropy probe (wmap)* observations: determination of cosmological parameters. *The Astrophysical Journal Supplement Series*, 148(1):175, 2003.

[25] Steen Hannestad. What is the lowest possible reheating temperature? *Physical Review D*, 70(4):043506, 2004.

[26] James Martin Overduin and Paul S Wesson. Dark matter and background light. *Physics reports*, 402(5-6):267–406, 2004.

[27] David N Spergel and Paul J Steinhardt. Observational evidence for self-interacting cold dark matter. *Physical Review Letters*, 84(17):3760, 2000.

[28] PJE Peebles. Large-scale background temperature and mass fluctuations due to scale-invariant primeval perturbations. 1982.

[29] JR Bond. Jr bond and as szalay, astrophys. j. 274, 443 (1983). *Astrophys. J.*, 274:443, 1983.

[30] Vijay K Narayanan, David N Spergel, Romeel Davé, and Chung-Pei Ma. Constraints on the mass of warm dark matter particles and the shape of the linear power spectrum from the lyα forest. *The Astrophysical Journal Letters*, 543(2):L103, 2000.

[31] Jesper Sommer-Larsen and Alexandre Dolgov. Formation of disk galaxies: warm dark matter and the angular momentum problem. *The Astrophysical Journal*, 551(2):608, 2001.

[32] Niayesh Afshordi, P McDonald, and DN Spergel. Primordial black holes as dark matter: the power spectrum and evaporation of early structures. *The Astrophysical Journal Letters*, 594(2):L71, 2003.

[33] Jeremiah P Ostriker and Paul Steinhardt. New light on dark matter. *Science*, 300(5627):1909–1913, 2003.

[34] Wayne Hu, Rennan Barkana, and Andrei Gruzinov. Fuzzy cold dark matter: the wave properties of ultralight particles. *Physical Review Letters*, 85(6):1158, 2000.

[35] Scott Tremaine and James E Gunn. Dynamical role of light neutral leptons in cosmology. *Physical Review Letters*, 42(6):407, 1979.

[36] Nils Bergvall, Erik Zackrisson, B-G Andersson, Daniel Arnberg, Josefa Masegosa, and Göran Östlin. First detection of lyman continuum escape from a local starburst galaxy-i. observations of the luminous blue compact galaxy haro 11 with the far ultraviolet spectroscopic explorer (fuse). *Astronomy & Astrophysics*, 448(2):513–524, 2006.

[37] DS Akerib, PD Barnes Jr, DA Bauer, PL Brink, B Cabrera, DO Caldwell, RM Clarke, A Da Silva, AK Davies, BL Dougherty, et al. Preliminary limits on the wimp-nucleon cross section from the cryogenic dark matter search (cdms). *Nuclear Physics B-Proceedings Supplements*, 70(1-3):64–68, 1999.

[38] Cheongho Han and Andrew Gould. Stellar contribution to the galactic bulge microlensing optical depth. *The Astrophysical Journal*, 592(1):172, 2003.

[39] Sean G Ryan, Timothy C Beers, Keith A Olive, Brian D Fields, and John E Norris. Primordial lithium and big bang nucleosynthesis. *The Astrophysical Journal Letters*, 530(2):L57, 2000.

[40] PAR Planck Collaboration, N Aghanim, M Arnaud, M Ashdown, J Aumont, C Baccigalupi, AJ Banday, RB Barreiro, JG Bartlett, et al. Astronomy & astrophysics (a&a). *A&A*, 594:A13, 2016.

[41] Alec Habig et al. An indirect search for wimps with super-kamiokande. *arXiv preprint hep-ex/0106024*, 2001.

[42] Gerard Jungman. G. jungman, m. kamionkowski, and k. griest, phys. rep. 267, 195 (1996). *Phys. Rep.*, 267:195, 1996.

[43] Lars Bergström. Non-baryonic dark matter: observational evidence and detection methods. *Reports on Progress in Physics*, 63(5):793, 2000.

[44] E Aliu, S Andringa, S Aoki, J Argyriades, K Asakura, R Ashie, H Berns, H Bhang, A Blondel, S Borghi, et al. Evidence for muon neutrino oscillation in an accelerator-based experiment. *Physical review letters*, 94(8):081802, 2005.

[45] Gianfranco Bertone, Dan Hooper, and Joseph Silk. Particle dark matter: Evidence, candidates and constraints. *Physics Reports*, 405(5-6):279–390, 2005.

[46] Eiichiro Komatsu, J Dunkley, MR Nolta, CL Bennett, B Gold, G Hinshaw, N Jarosik, D Larson, M Limon, L Page, et al. Five-year wilkinson microwave anisotropy probe* observations: cosmological interpretation. *The Astrophysical Journal Supplement Series*, 180(2):330, 2009.

[47] Simon DM White, Julio F Navarro, August E Evrard, and Carlos S Frenk. The baryon content of galaxy clusters: a challenge to cosmological orthodoxy. *nature*, 366(6454):429, 1993.

[48] Tom Banks, Michael Dine, Patrick J Fox, and Elie Gorbatov. On the possibility of large axion decay constants. *Journal of Cosmology and Astroparticle Physics*, 2003(06):001, 2003.

[49] Roberto D Peccei and Helen R Quinn. Cp conservation in the presence of pseudoparticles. *Physical Review Letters*, 38(25):1440, 1977.

[50] Georg G Raffelt. Astrophysical axion bounds. In *Axions*, pages 51–71. Springer, 2008.

[51] Jonathan L Feng, Jean-François Grivaz, and Jane Nachtman. Searches for supersymmetry at high-energy colliders. In *Perspectives on Supersymmetry II*, pages 351–419. World Scientific, 2010.

[52] Lars Bergström. Dark matter candidates. *New Journal of Physics*, 11(10):105006, 2009.

[53] B Ryden. Introduction to cosmology. introduction to cosmology/barbara ryden. 2003.

[54] Julio F Navarro. The structure of cold dark matter halos. 171:255–258, 1996.

[55] Marco Cirelli. Status of indirect (and direct) dark matter searches. *arXiv preprint arXiv:1511.02031*, 2015.

[56] Teresa Marrodan Undagoitia and Ludwig Rauch. Dark matter direct-detection experiments. *Journal of Physics G: Nuclear and Particle Physics*, 43(1):013001, 2015.

[57] Pran Nath, Brent Nelson, Hooman Davoudiasl, Bhaskar Dutta, Daniel Feldman, Zuowei Liu, Tao Han, Paul Langacker, Rabi Mohapatra, Jose Valle, et al. The hunt for new physics at the large hadron collider. *Nuclear Physics B-Proceedings Supplements*, 200:185–417, 2010.

[58] Ben C Allanach, Christopher Gorham Lester, M Andy Parker, and Bryan R Webber. Measuring sparticle masses in non-universal string inspired models at the lhc. *Journal of High Energy Physics*, 2000(09):004, 2000.

[59] Leszek Roszkowski, Roberto Ruiz de Austri, and Ki-Young Choi. Gravitino dark matter in the cmssm and implications for leptogenesis and the lhc. *Journal of High Energy Physics*, 2005(08):080, 2005.

[60] Andreas Birkedal, Konstantin T Matchev, Maxim Perelstein, and Andrew Spray. Robust gamma ray signature of wimp dark matter. *arXiv preprint hep-ph/0507194*, 2005.

[61] JD Lewin and PF Smith. Review of mathematics, numerical factors, and corrections for dark matter experiments based on elastic nuclear recoil. *Astroparticle Physics*, 6(1):87–112, 1996.

[62] Michael Klasen, Martin Pohl, and Günter Sigl. Indirect and direct search for dark matter. *Progress in Particle and Nuclear Physics*, 85:1–32, 2015.

[63] A Abramowski, F Aharonian, F Ait Benkhali, AG Akhperjanian, E Angüner, M Backes, S Balenderan, A Balzer, Anna Barnacka, Yvonne Becherini, et al. Search for dark matter annihilation signatures in hess observations of dwarf spheroidal galaxies. *Physical Review D*, 90(11):112012, 2014.

[64] Luca Quartuccio, Chiara Baldini, Elena Bartoloni, Roberta Priori, Francesco Carubbi, Laura Corazza, Alessia Alunno, Serena Colafrancesco, Nicoletta Luciano, Roberto Giacomelli, et al. Anti-ssa/ssb-negative sjögren's syndrome shows a lower prevalence of lymphoproliferative manifestations, and a lower risk of lymphoma evolution. *Autoimmunity reviews*, 14(11):1019–1022, 2015.

[65] Emma Storm. *Nonthermal Emission from Galaxy Clusters*. University of California, Santa Cruz, 2015.

[66] HJ Völk. The correlation between radio and far-infrared emission for disk galaxies-a calorimeter theory. *Astronomy and Astrophysics*, 218:67–70, 1989.

[67] Min S Yun, Naveen A Reddy, and James J Condon. Radio properties of infrared-selected galaxies in the iras 2 jy sample. *The Astrophysical Journal*, 554(2):803, 2001.

[68] Markus Ackermann, Marco Ajello, A Allafort, Luca Baldini, Jean Ballet, D Bastieri, K Bechtol, R Bellazzini, B Berenji, ED Bloom, et al. Gev observations of star-forming galaxies with the fermi large area telescope. *The Astrophysical Journal*, 755(2):164, 2012.

[69] P Blasi and Sergio Colafrancesco. High energy phenomena in clusters of galaxies. *Nuclear Physics B-Proceedings Supplements*, 70(1-3):495–499, 1999.

[70] S Colafrancesco and P Marchegiani. On the inverse compton scattering interpretation of the hard x-ray excesses in galaxy clusters: the case of ophiuchus. *Astronomy & Astrophysics*, 502(3):711–719, 2009.

[71] Tesla E Jeltema and Stefano Profumo. Implications of fermi observations for hadronic models of radio halos in clusters of galaxies. *The Astrophysical Journal*, 728(1):53, 2011.

[72] Emma Storm, Tesla E Jeltema, Stefano Profumo, and Lawrence Rudnick. Constraints on dark matter annihilation in clusters of galaxies from diffuse radio emission. *The Astrophysical Journal*, 768(2):106, 2013.

[73] Paolo Marchegiani and Sergio Colafrancesco. The role of dark matter subhalos in the non-thermal emission of galaxy clusters. *Journal of Cosmology and Astroparticle Physics*, 2016(11):033, 2016.

[74] Markus Ackermann, M Ajello, A Albert, A Allafort, WB Atwood, Luca Baldini, J Ballet, G Barbiellini, D Bastieri, K Bechtol, et al. Search for cosmic-ray-induced gamma-ray emission in galaxy clusters. *The Astrophysical Journal*, 787(1):18, 2014.

[75] B Huber, C Tchernin, D Eckert, Christian Farnier, A Manalaysay, U Straumann, and R Walter. Probing the cosmic-ray content of galaxy clusters by stacking fermi-lat count maps. *Astronomy & Astrophysics*, 560:A64, 2013.

[76] Franco Vazza and Marcus Brueggen. Do radio relics challenge diffusive shock acceleration? *Monthly Notices of the Royal Astronomical Society*, 437(3):2291–2296, 2013.

[77] B Dennison. Formation of radio halos in clusters of galaxies from cosmic-ray protons. *The Astrophysical Journal*, 239:L93–L96, 1980.

[78] Pasquale Blasi and Sergio Colafrancesco. Cosmic rays, radio halos and nonthermal x-ray emission in clusters of galaxies. *Astroparticle Physics*, 12(3):169–183, 1999.

[79] Sergio Colafrancesco and Barbara Melé. Neutralinos and the origin of radio halos in clusters of galaxies. *The Astrophysical Journal*, 562(1):24, 2001.

[80] Luigina Feretti, Gabriele Giovannini, Federica Govoni, and Matteo Murgia. Clusters of galaxies: observational properties of the diffuse radio emission. *The Astronomy and Astrophysics Review*, 20(1):54, 2012.

[81] Markus Ackermann, A Albert, Brandon Anderson, L Baldini, J Ballet, G Barbiellini, D Bastieri, K Bechtol, R Bellazzini, E Bissaldi, et al. Dark matter constraints from observations of 25 milky way satellite galaxies with the fermi large area telescope. *Physical Review D*, 89(4):042001, 2014.

[82] AA Abdo, Markus Ackermann, Marco Ajello, WB Atwood, Luca Baldini, J Ballet, Guido Barbiellini, D Bastieri, BM Baughman, K Bechtol, et al. Fermi large area telescope view of the core of the radio galaxy centaurus a. *The Astrophysical Journal*, 719(2):1433, 2010.

[83] Paolo Gondolo, Joakim Edsjö, Piero Ullio, Lars Bergström, Mia Schelke, and Edward A Baltz. Darksusy: Computing supersymmetric dark matter properties numerically. *Journal of Cosmology and Astroparticle Physics*, 2004(07):008, 2004.

[84] Federico Sembolini, Gustavo Yepes, Marco De Petris, Stefan Gottlöber, Luca Lamagna, and Barbara Comis. The music of galaxy clusters–i. baryon properties and scaling relations of the thermal sunyaev–zel'dovich effect. *Monthly Notices of the Royal Astronomical Society*, 429(1):323–343, 2012.

[85] Paolo Gondolo and Graciela Gelmini. Cosmic abundances of stable particles: Improved analysis. *Nuclear Physics B*, 360(1):145–179, 1991.

[86] Malcolm S Longair. High energy astrophysics: vol. 1. *Comments on Astrophysics*, 17:259–261, 1994.

[87] Volker Springel. Smoothed particle hydrodynamics in astrophysics. *Annual Review of Astronomy and Astrophysics*, 48:391–430, 2010.

[88] Federico Sembolini, G Yepes, M De Petris, S Gottlöber, L Lamagna, and B Comis. The evolution of the y–m scaling relation in music clusters. *Astronomische Nachrichten*, 334(4-5):441–444, 2013.

[89] Ilias Cholis, Carmelo Evoli, Francesca Calore, Tim Linden, Christoph Weniger, and Dan Hooper. The galactic center gev excess from a series of leptonic cosmic-ray outbursts. *Journal of Cosmology and Astroparticle Physics*, 2015(12):005, 2015.

[90] Andreas Burkert. The structure of dark matter halos in dwarf galaxies. *The Astrophysical Journal Letters*, 447(1):L25, 1995.

[91] Federico Sembolini, Gustavo Yepes, Marco De Petris, Stefan Gottlöber, Luca Lamagna, and Barbara Comis. Erratum: The music of galaxy clusters-i. baryon properties and scaling relations of the thermal sunyaev-zel'dovich effect. *Monthly Notices of the Royal Astronomical Society*, 434:2718–2719, 2013.

DECLARATION

ADDIS ABABA UNIVERSITY
COLLEGE OF NATURAL AND COMPUTATIONAL SCIENCES
DEPARTMENT OF PHYSICS

MSc Thesis

Gamma-ray Emission From Dark Matter Annihilation Process In Simulated Coma Like Galaxy Cluster

Name of Candidate: Goshu Woldeyesus Damte

I the under signed declare that the thesis is my original work and no part of it can be claimed as an intellectual property of anybody else except me and my advisors.

Signature: ______________________